Pacific Northwest
NATIONAL LABORATORY

PNNL-29815

Foam Degradation Model during Thermal Hypothetical Accident Conditions

April 2020

Sarah Suffield
James Fort

U.S. DEPARTMENT OF ENERGY

Prepared for the U.S. Department of Energy
under Contract DE-AC05-76RL01830

DISCLAIMER

PACIFIC NORTHWEST NATIONAL LABORATORY
operated by
BATTELLE
for the
UNITED STATES DEPARTMENT OF ENERGY
under Contract DE-AC05-76RL01830

Printed in the United States of America

Available to DOE and DOE contractors from the Office of Scientific and Technical Information,
P.O. Box 62, Oak Ridge, TN 37831-0062
www.osti.gov
ph: (865) 576-8401
fax: (865) 576-5728
email: reports@osti.gov

Available to the public from the National Technical Information Service
5301 Shawnee Rd., Alexandria, VA 22312
ph: (800) 553-NTIS (6847)
or (703) 605-6000
email: info@ntis.gov
Online ordering: http://www.ntis.gov

PNNL-29815

Foam Degradation Model during Thermal Hypothetical Accident Conditions

April 2020

Sarah Suffield
James Fort

Prepared for
the U.S. Department of Energy
under Contract DE-AC05-76RL01830

Pacific Northwest National Laboratory
Richland, Washington 99354

Summary

Current practice in Safety Analysis Report for Packaging (SARP) thermal analysis for hypothetical accident conditions (HAC) of packages is to not explicitly model the consequence to the foam impact limiting material, but instead to make conservative estimates of those consequences and begin calculations from that point. This approach is typically used for the foam regression distance, which is the thickness of the degraded foam layer after the 30-minute fire event. Estimates for regression distance can come directly from package burn test results or from correlations based on one-dimensional testing by the foam manufacturer. In either case, this is a subjective process, and although it can be used to produce a conservative result, it is a significant approximation in the analysis.

This paper describes testing and refinement of a simplified foam regression model. Comparisons are made against available data from laboratory experiments. Model refinements were tested until satisfactory agreement was achieved. The final modeling approach was then compared with post-test inspection results from HAC burn test data. A new model with an effective thermal conductivity based on foam to char density variation was shown successful in representing laboratory-scale foam thermal degradation experiments and full-scale burn tests of a current package. This model offers a technically defensible and predictive approach for modeling thermal degradation of rigid polyurethane insulation in transport packages.

Acknowledgments

This work was funded by the National Nuclear Security Administration (NNSA) Office of Infrastructure Operations and Modernization (NA-522) under U.S. Department of Energy Contract DE-AC05-76RL01830. Technical direction and oversight of the work is conducted by the NNSA Office of Packaging and Transportation (NA-531).

Acronyms and Abbreviations

APDL	ANSYS Parametric Design Language
CAD	computer aided design
CV	containment vessel
DPP-3	Defense Programs Package - 3
FEM	finite element method
FVM	finite volume method
HAC	hypothetical accident conditions
OPT	Office of Packaging and Transportation
PNNL	Pacific Northwest National Laboratory
SARP	Safety Analysis Report for Packaging
SNL	Sandia National Laboratories
TGA	thermogravimetric analysis

Contents

Figures

Tables

1.0 Introduction

It would be beneficial to move toward a more predictive modeling strategy for foam property change under HAC thermal conditions to provide a more accurate and defensible analysis result. A detailed investigation of rigid polyurethane foam behavior in fire conditions was conducted by Sandia National Laboratories (SNL) from 1995 to 2000. This work was documented in a series of reports and conference papers, culminating with a summary journal article which discussed select experimental measurements and a comparison with model predictions. Laboratory tests included foam recession in a simple one-dimensional experiment consisting of a cylindrical foam test sample that was subjected to a heat flux at one end representative of fire conditions. In subsequent experiments, a stainless- steel dummy component was embedded in the same foam geometry. The initial test (Chu, et al., 1996) was performed with 6 lb/ft^3 (96 kg/m^3) General Plastics FR-3706 foam. Later testing (Chu, et al., 1999) included foam densities up to 22 lb/ft^3 (353 kg/m^3), although the foam manufacturer is not specified. Test data included temperatures from embedded thermocouples and X-ray images showing the developing foam/char boundary. These tests also included detailed analytical work to understand the chemical changes undergone by the foam during this transition (Hobbs, Erickson, and Chu, 2000). Detailed models based on this understanding were used to predict foam regression in HAC thermal conditions (Hobbs, Erickson, and Chu, 2000). While these models accurately represented measured temperatures and rate of foam regression in the SNL experiments, the models are complex and not practical for SARP calculations.

For SARP purposes, a less detailed modeling approach is desired that still provides reasonable predictive accuracy for the foam-char boundary. Initial results from a simplified model of the 9977 burn test suggest that acceptable results may not require such detail. Model results gave a reasonable match with foam regression observed in 9977 post-test inspections. However, the modeling approach needed further evaluation to determine its applicability to other packages.

This paper describes testing and refinement of a simplified foam regression model. Comparisons are made against available data from the SNL experiments. Model refinements were tested until satisfactory agreement was achieved. The final modeling approach was then compared with post-test inspection results from the 9977 burn test data.

2.0 ANSYS Foam Degradation Model – SNL Experiment #1

An ANSYS APDL model was constructed to look at the degradation of rigid polyurethane foam when exposed to a fire. The model simulated an experiment run by SNL to investigate the fire-induced response of a closed cell rigid polyurethane foam (Chu, et al., 1996). The experiment placed a foam sample in a cylindrical test vessel and exposed it to a simulated fire condition by heating the bottom of the test vessel to 1283 K (1850°F) using a radiant heat source. Provision was also made in this test to pressurize the system, but only the ambient pressure data is of interest here. The test configuration is shown schematically in Figure 1. General Plastics Last-A-Foam FR3706 was used for the foam sample. This foam has a density of 6 lb/ft^3 (96 kg/m^3). Thermocouples embedded in the foam sample captured the thermal response of the foam. The resulting temperatures are shown in Figure 2. The number associated with each temperature curve in the plot is the thermocouple location (in mm) relative to the surface of the foam sample.

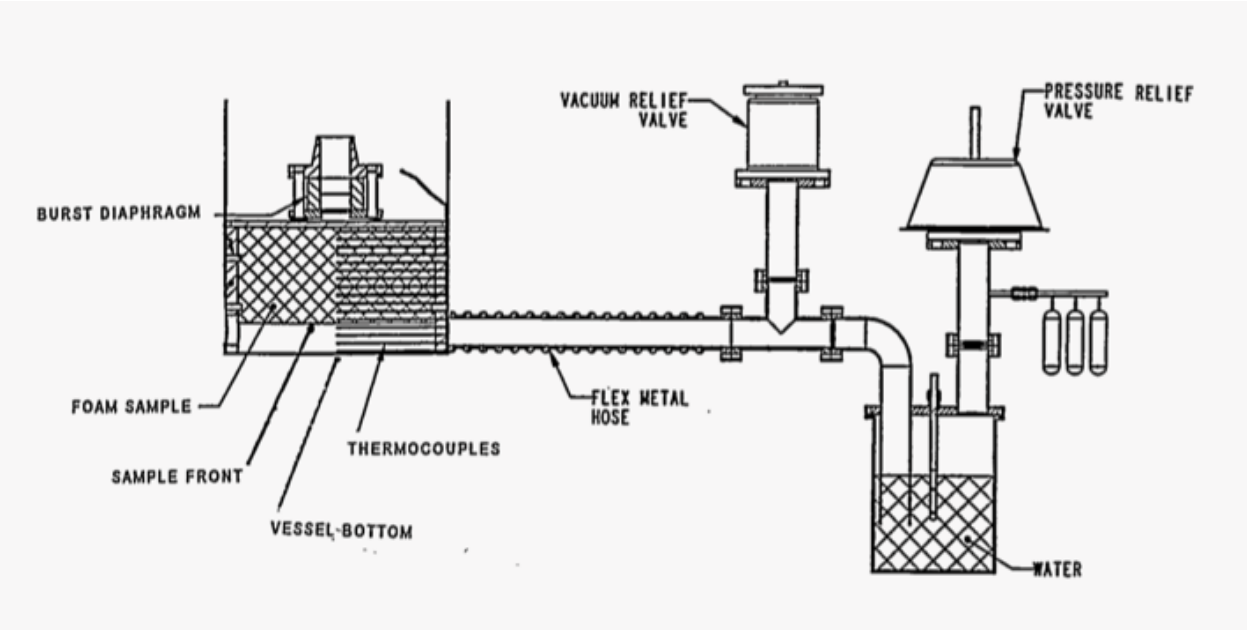

Figure 1. Experimental configuration used in Chu, et al. 1996 (this is Fig. 1 in that reference).

The heated period is described in the report (Chu 1996) as lasting 1320 seconds. “It took ~200 s for the vessel bottom to reach the testing temperature of 1283K.” Based on the test results shown in Figure 2, it is assumed that the lamps were turned on at 130 seconds, at the start of the linear ramp-up in the surface temperature, and turned off at 1450 seconds, which is when the surface temperature begins to fall off.

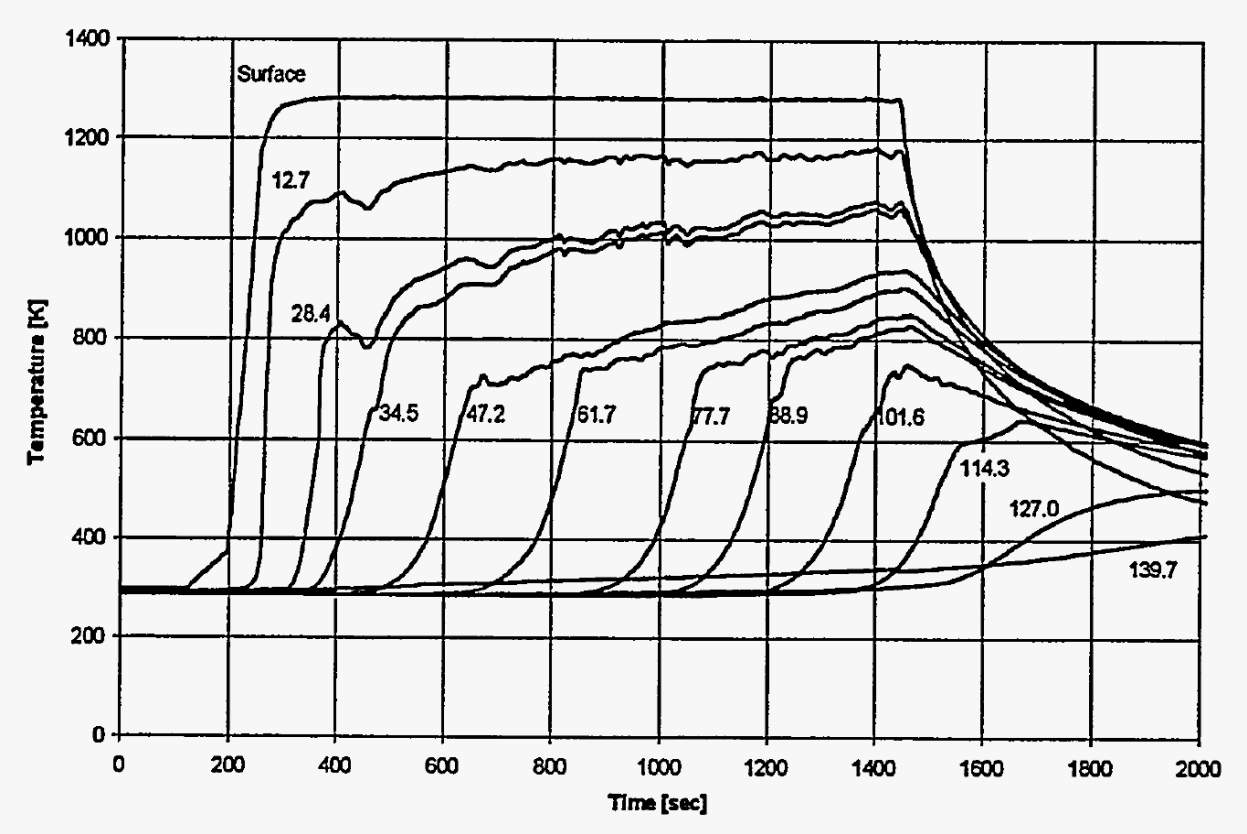

Figure 2. Temperature of the vessel bottom and in-depth temperature of the foam layer (numbers associated with temperature traces show depth in mm from front surface of foam sample.

2.1 Initial Model

An initial model was created using ANSYS APDL to replicate the SNL foam experiment. Geometry for the model was constructed using the commercial computer aided design (CAD) program SolidWorks, and then imported into the utility ANSYS Mesh. A discretized form of each solid region and each interior gas space was generated. A conformal interface was established across all internal boundaries between parts, which constitute shared nodes along any part-to-part boundary. Figure 3 shows a cross-sectional view of the CAD geometry. The foam is shown in green, the stainless-steel canister is shown in gray, and the gap region between the foam and canister base is shown in yellow. The gap region is filled with air. Figure 4 shows an overall and cross-sectional view of the mesh. The mesh contains hexahedral and wedge elements.

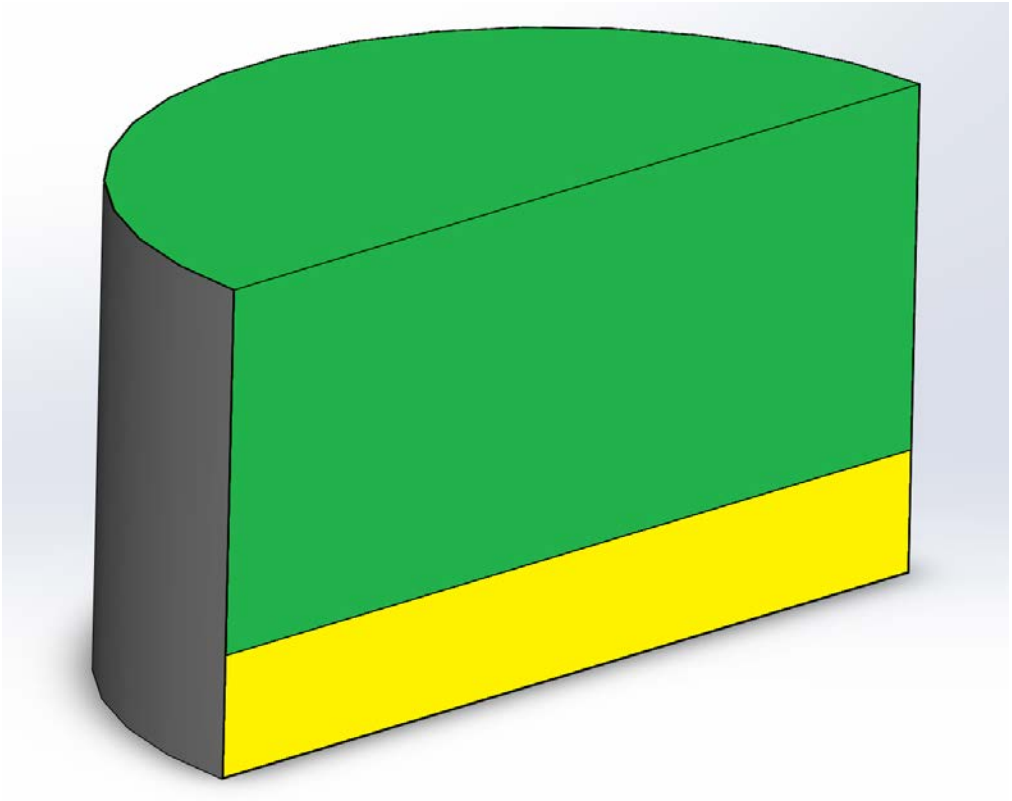

Figure 3. Cross-sectional view through the center of the canister assembly geometry.

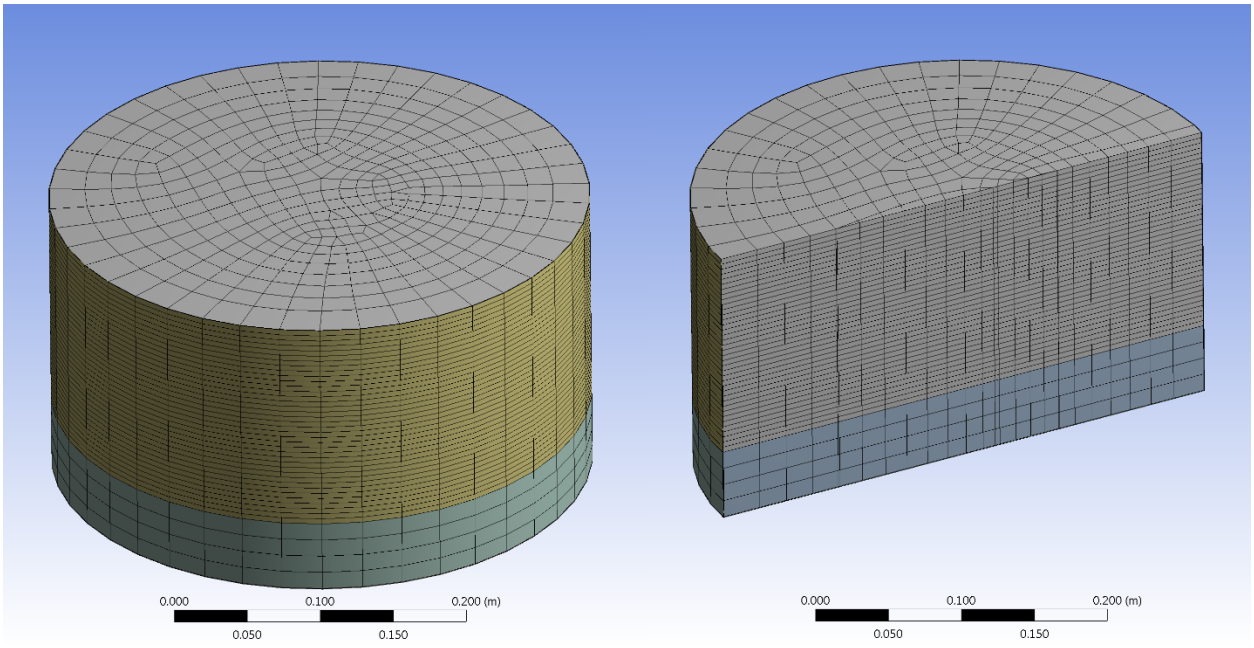

Figure 4. Overall and cross-sectional view of the canister assembly mesh.

Tables 1-2 list the material properties for the stainless-steel canister and the foam sample. The emissivity values used in the model are shown in Table 3.

Table 1. Stainless-steel material properties (Incropera et al., 2007).

Temperature [K]	Thermal Conductivity [W/m-K]	Specific Heat [J/kg-K]	Density [kg/m^3]
100	9.2	272	7920
200	12.6	402	
300	14.9	477	
400	16.6	515	
600	19.8	557	
800	22.6	582	

Table 2. Foam material properties (General Plastics, 1991).

Thermal Conductivity [W/m-K]	Specific Heat [J/kg-K]	Density [kg/m^3]
0.034615	1478	96

Table 3. Emissivity.

Material	Emissivity
Stainless Steel[1]	0.46
Foam	0.9

Free convection to ambient air from external surfaces of the canister and foam was calculated using natural convection correlations from the *Handbook of Applied Thermal Design* (Guyer, 1989) for the following surface geometries:

- Vertical cylinder (cylindrical sides of canister outer shell).
- Horizontal surface upward facing (top of canister, top of foam).

Thermal radiation between the environment and canister was also included in the model. An ambient temperature of 60 °F (15.6 °C) was applied at all exterior environment nodes. Internal surface-to-surface radiation was included for the air cavity region within the model using radiation matrices with view factors created by raytracing. The emissivity values listed in Table 3 were applied along the exposed surfaces within the air region.

A transient analysis was run. At the start of the analysis an 1850 °F (1283 K) temperature boundary was applied along the bottom surface of the canister. This was to simulate the radiant heat source applied along the base of the canister. The heating phase of the experiment lasted for 1320 seconds (22 minutes). After 1320 seconds the temperature boundary along the base of the canister was changed to a natural convection boundary with thermal radiation to the

[1] Test vessel preheated to 870 K (1107°F) prior to test to provide consistent oxide layer (Chu, et al., 1996).

surroundings and the transient analysis was continued out to 2000 seconds to capture the cooldown of the experiment.

The resulting predicted temperatures from the initial ANSYS model for the heated part of the transient are shown in Figure 5. The predicted temperatures are very different from the measurements, both in magnitude and rate of change. To rule out modeling errors, a comparison was first made with an independent model. That testing is described below.

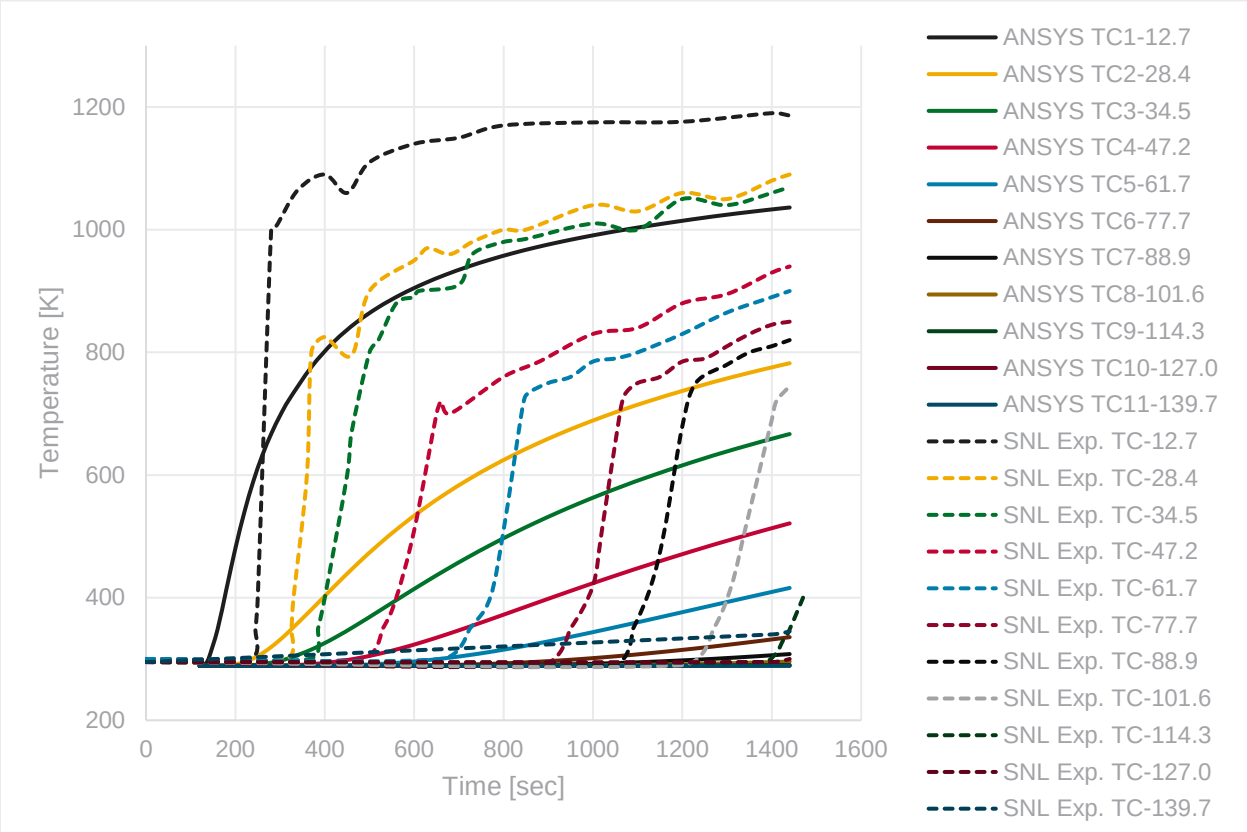

Figure 5. Thermocouple response compared to predicted temperatures – initial ANSYS model.

2.2 STAR-CCM+ Model Comparison

An identical model was created with the commercial computational fluid dynamics code STAR-CCM+ (Siemens, 2016)). Temperature contour plots at the end of the heating phase are shown in Figures 6 and 7 for both the ANSYS and STAR-CCM+ model. Figure 8 plots the thermal response of thermocouple #1 (at the 12.7 mm location) for both models.

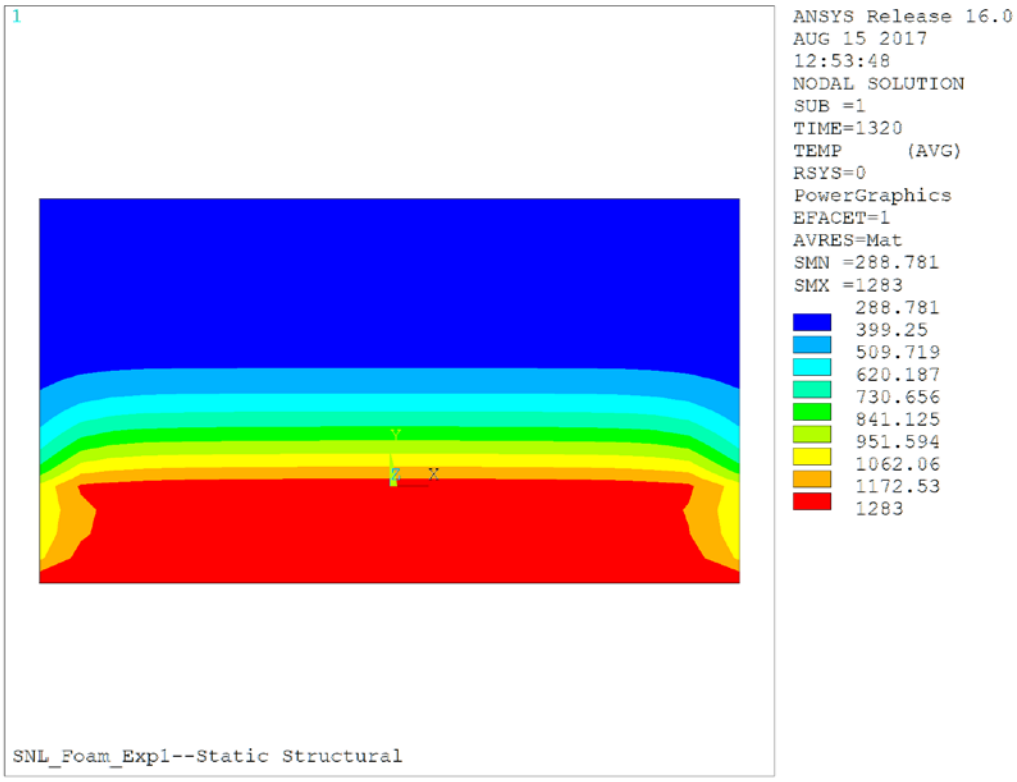

Figure 6. Temperature contour plot at 1320s – ANSYS model (temperatures shown in K).

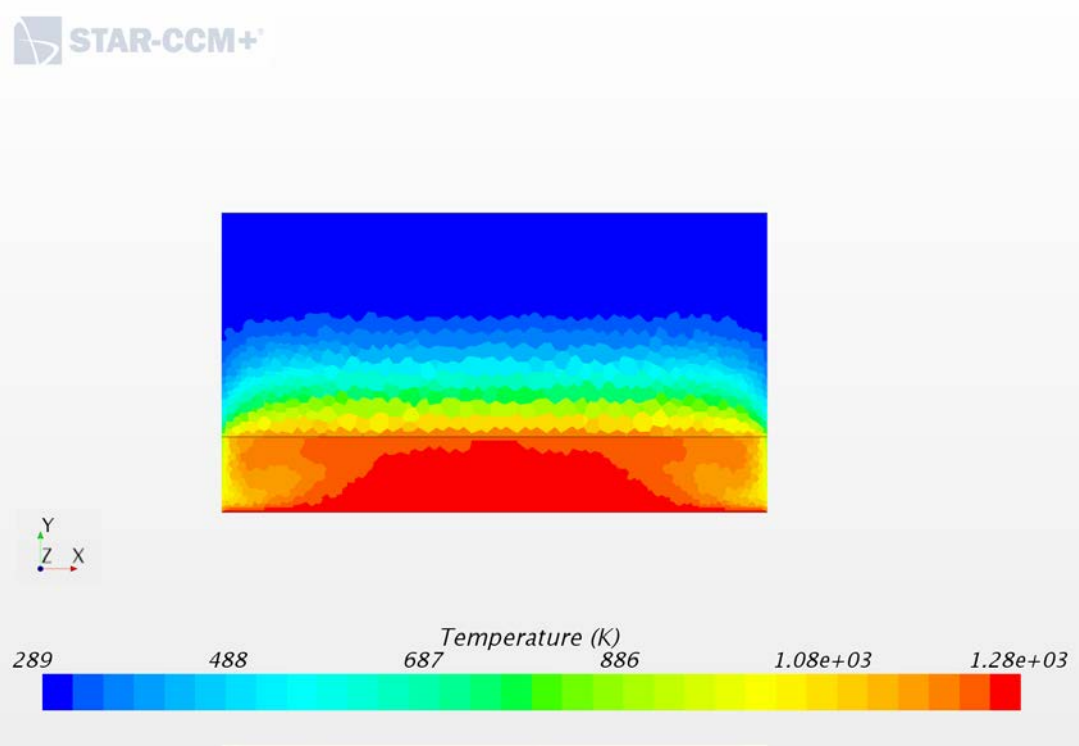

Figure 7. Temperature contour plot at 1320s – STAR-CCM+ model (temperatures shown in K).

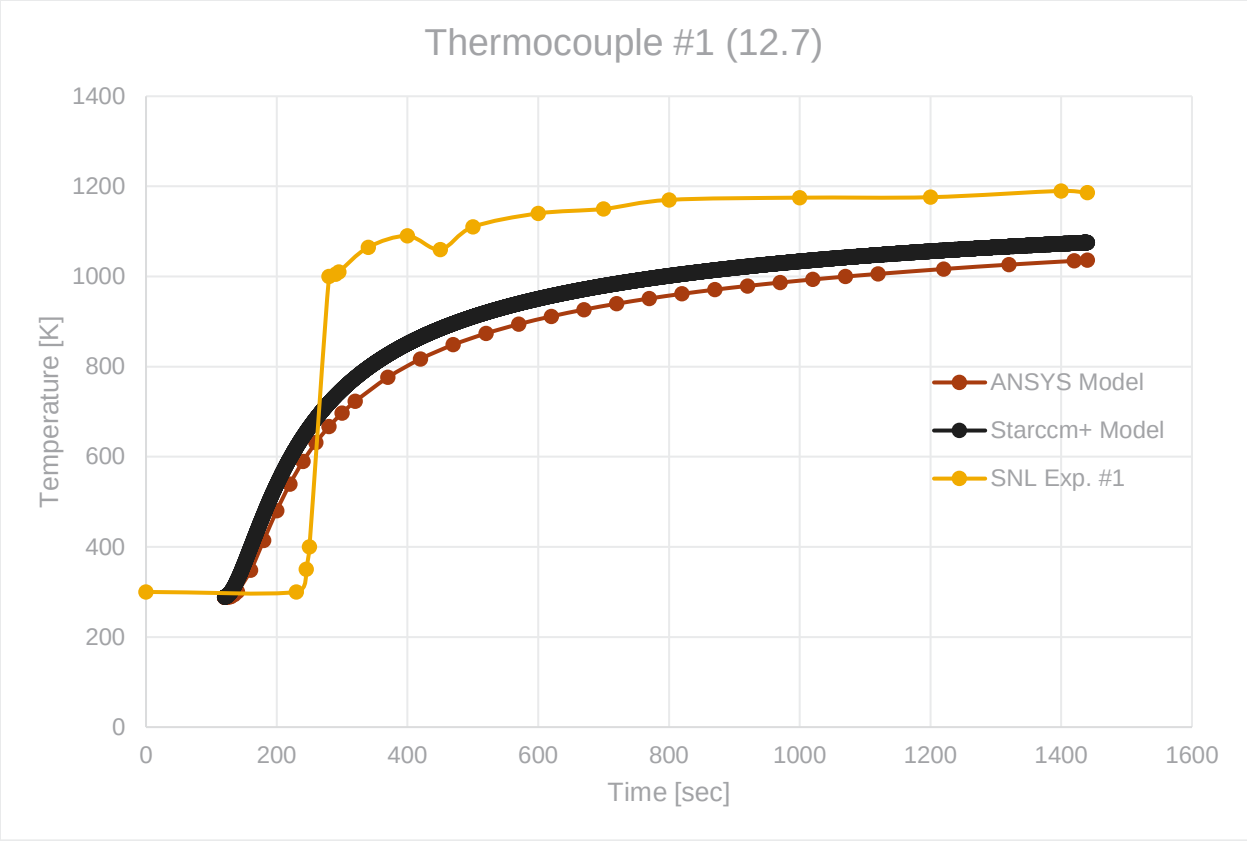

Figure 8. Thermal response of thermocouple #1 (at the 12.7 mm location) compared to model results.

Figures 6 through 8 show a good comparison between ANSYS and STAR-CCM+ models. When compared with the experiment results from Figure 2, the models are not accurately capturing the thermal response of the foam. As the foam is exposed to higher temperatures, it will burn and char. Additional physics needed to be added to the model to try to accurately capture the effect on temperature rise due to charring of the foam.

2.3 Moving Foam Model

The principal mode of heat transfer from the heated canister base and foam is radiation. If the foam burns away as it heats up, the foam surface will recede. For this case, the initial ANSYS model was modified to adjust the foam surface during the transient analysis based on the average element layer temperature of the foam. The foam mesh is vertically divided into 38 element layers, and at each timestep the model computes the average temperature in each vertical element layer. If the average element temperature is greater than 1030 °F (554 °C), all elements in that layer are changed to air and the radiation surface for the foam is moved up to the next foam element layer. The 1030 °F temperature limit was chosen because it is higher than the 1000 °F autoignition temperature given for LAST-A-FOAM FR-3700 (General Plastics, 1991). The resulting temperatures for the modified “moving foam” model are shown in Figure 9.

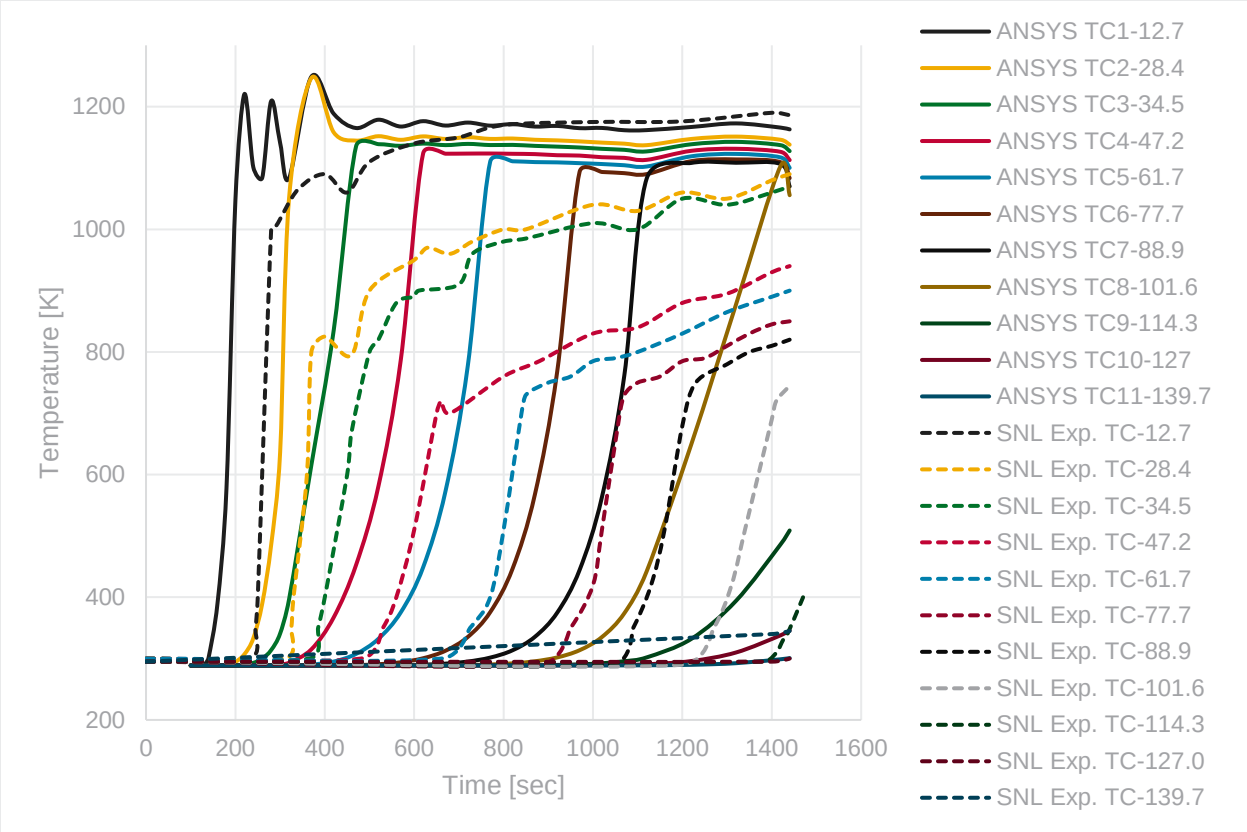

Figure 9. Thermocouple response – “moving foam” ANSYS model.

The temperatures plotted in Figure 9 show that the “moving foam” model overestimates the thermal response of the foam. Peak temperatures are too high, and the regression front is moving faster than indicated by the experiment results in Figure 2. This is most likely due to the assumption that the foam completely burns away and is replaced by air. In reality, the foam turns into char as it burns, leaving an intervening material between the heated surface and the virgin foam (Chu, et al., 1996).

2.4 Char Model with Default Parameters

For this case, the initial ANSYS model was modified to include a char material which replaced foam elements within a certain temperature range as the foam heats up. The previous “moving foam” model assumed that at the autoignition (1000 °F) temperature, the foam had been replaced by ash, and the space was predominately gas. It did not account for the foam to char transition, which happens at a lower temperature than the autoignition temperature limit. For the char model the foam elements are replaced with char once the elements reach a certain temperature limit, and without an oxygen source the char is not assumed to transition to ash. A 600 °F temperature limit was chosen based on the thermogravimetric analysis of Last-A-Foam and the temperature at which the foam samples were observed to form an intumescent char at the surface (General Plastics, 1991). At each timestep the model looks at the temperature for each element within the foam, and if the element temperature is greater than 600 °F (315 °C) the element material is changed to a char.

The material properties of char are based on a generalized pyrolysis model for combustible solids, including charring solids (Lautenberger & Fernandez-Pello, 2009). The pyrolysis model uses the following equations for the bulk density, specific heat, and effective thermal conductivity of the condensed species:

Effective Density $$\rho_{eff} = \rho_o \left(\frac{T}{T_r}\right)^{n_p}$$ Eq. 1

Effective Specific Heat $$c_{eff} = c_o \left(\frac{T}{T_r}\right)^{n_c}$$ Eq. 2

Effective Thermal Conductivity $$k_{eff} = k_o \left(\frac{T}{T_r}\right)^{n_k} + \gamma\sigma T^3$$ Eq. 3

Where;

T = temperature
Tr = reference temperature (usually 300K)
σ = Stefan Boltzmann constant

The pyrolysis model report (Lautenberger & Fernandez-Pello, 2009) presents coefficients for an intumescent coating. These are shown reproduced in Table 4. The Last-A-Foam FR-3700 series foam was developed to form an intumescent char which prevents smoldering of the foam and provides a high level of thermal protection (General Plastics, 1991). Using the values for char listed in Table 4 and equations 1 through 3, the effective char properties were calculated for the ANSYS model. The effective thermal conductivity was calculated using the average char element temperature.

Table 4. Condensed phase parameters for intumescent coating simulations (Lautenberger and Fernandez-Pello 2009).

Char						
K_o [W/mK]	$\mathbf{n_k}$	P_o [kg/m^3]	$\mathbf{n_p}$	C_o [J/kgK]	$\mathbf{n_c}$	Υ [m]
0.041	0.441	17.4	0	1640	0	0.003

Results for the modified ANSYS “char” model are shown in Figure 10. The results show that adding the char material improved the response of the foam at the two thermocouple locations nearest the heated surface (Figure 2), but temperatures at more deeply embedded thermocouple locations lag significantly behind the measured values.

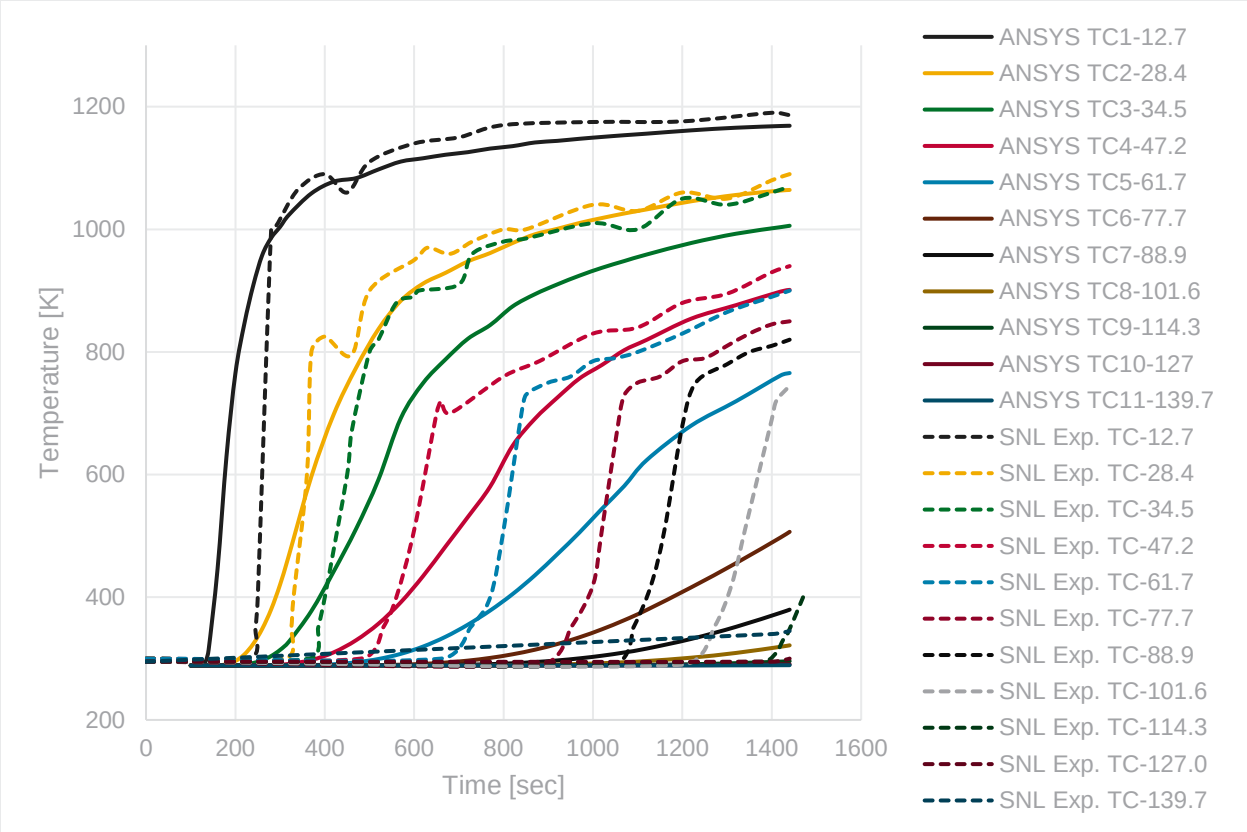

Figure 10. Thermocouple response – “char” ANSYS model.

2.5 Char Model with Variable Gamma

In porous media at higher temperatures, one example being fiber insulation (Litovsky, et al., 2008), thermal radiation can become the dominant mode of heat transfer. This behavior should be expected for the Last-A-Foam char layer. The second term given in equation 3 (for effective thermal conductivity) accounts for radiation heat transfer across pores. The leading coefficient on that term, γ (gamma), is used by Lautenberger and Fernandez-Pello (2009) as a material dependent constant. To model the expected increase in thermal radiation through the pore space from a relatively dense virgin foam to a less dense char, a variable gamma formulation is proposed.

The ANSYS “char” model was modified to incorporate a variable γ term in equation 3 for the effective char thermal conductivity. The assumption made here is that γ should increase as the foam solid phase breaks down and the char becomes more porous, which should coincide with the decrease in material density. Figure 11 plots the change in weight percent of foam as a function of temperature from a thermogravimetric analysis (TGA) (General Plastics, 1991).

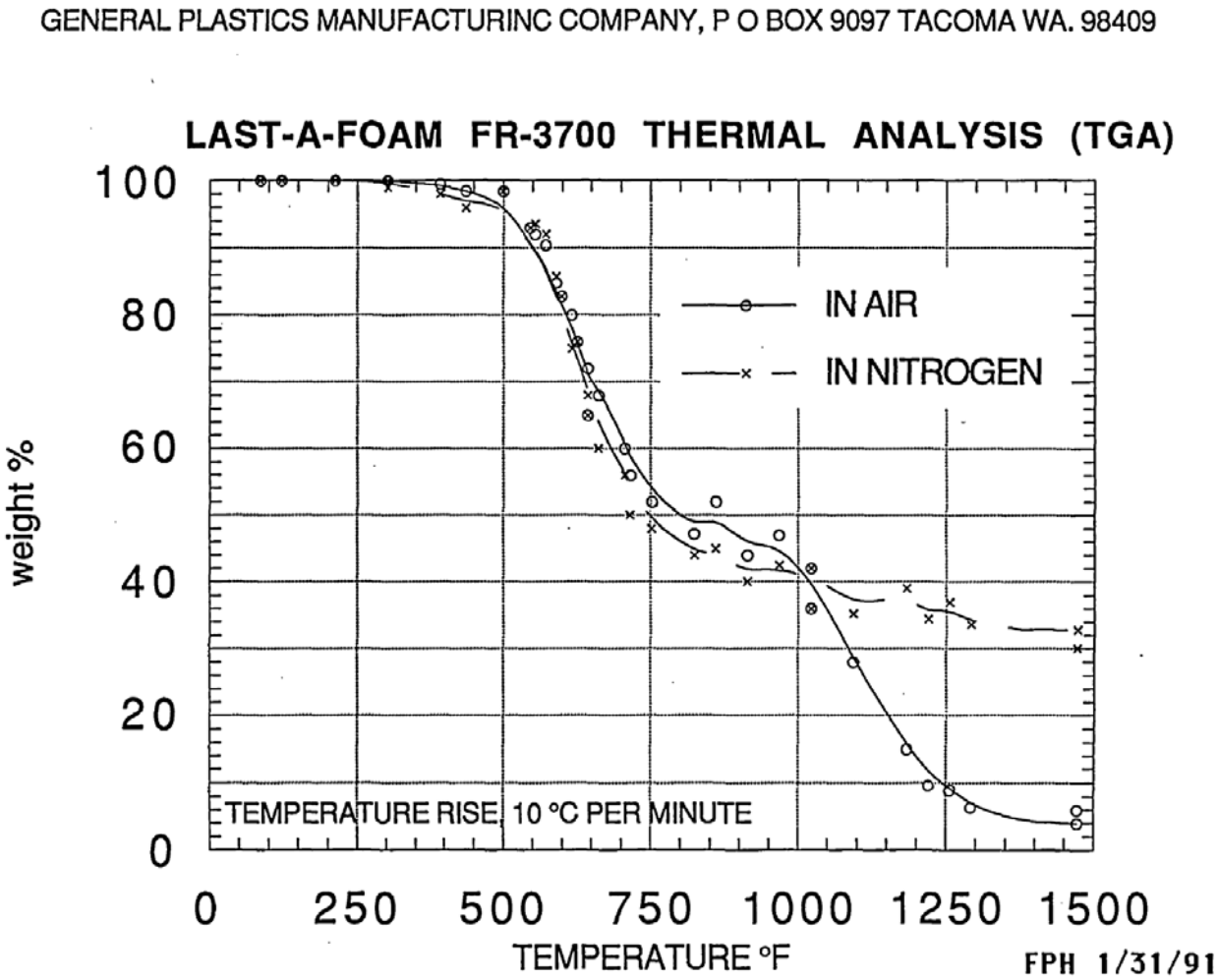

Figure 11. Last-A-Foam FR-3700 thermogravimetric analysis (General Plastics, 1991).

In developing a model for foam pyrolysis, the “in nitrogen” data was selected from Figure 11. The curve shown in Figure 12 was constructed by subtracting the “in nitrogen” weight fraction from 1 and scaling the resulting value to be consistent with the γ value listed in Table 4 (0.003). Subtracting the weight fraction of foam from 1 represents the fraction of void space within the foam, with a value of 1 representing no foam left. The void fraction curve was scaled to a γ value of 0.003 by dividing the void fraction by 100. This resulted in a value of 0.003 at 650 °F. Since the description of the TGA noted that at 600 °F the entire surface of each foam sample was covered with a continuous char (General Plastics, 1991), a value of 0.003 at 650 °F seems reasonable.

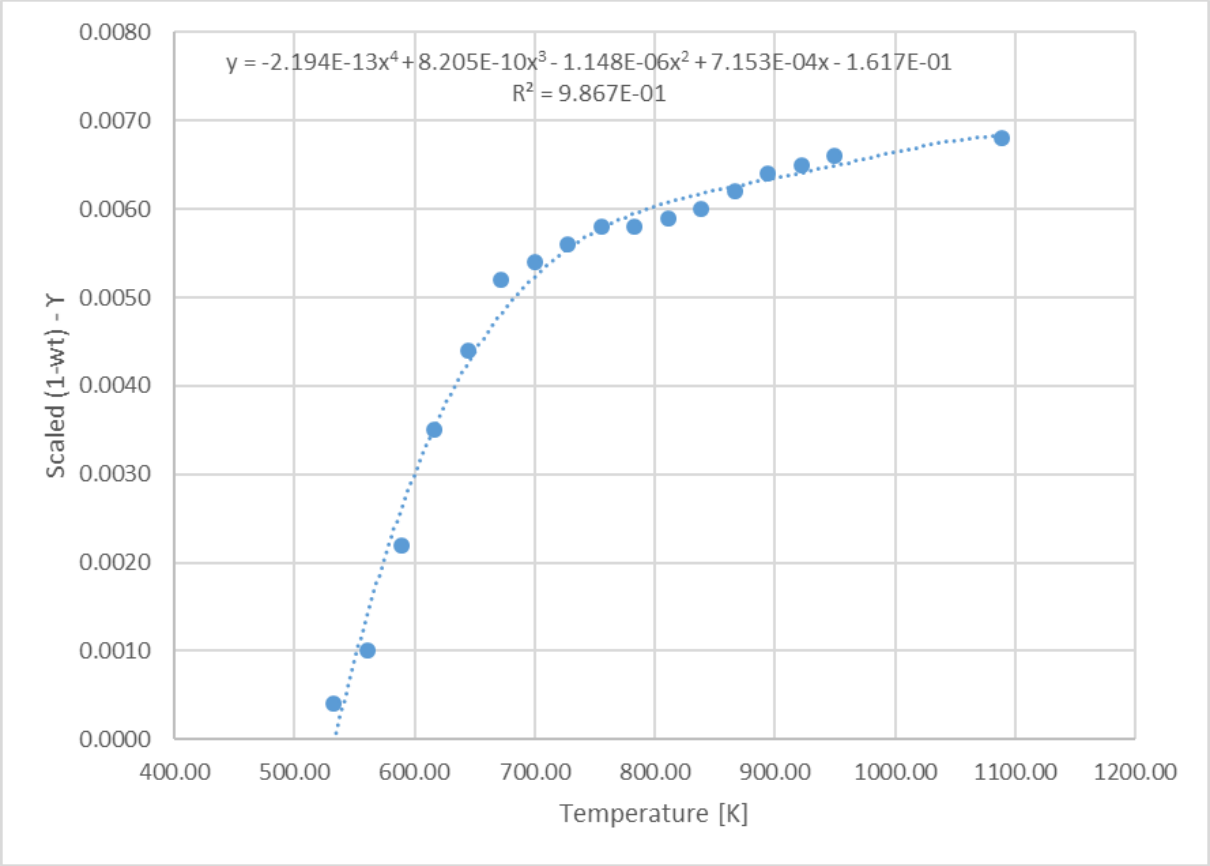

Figure 12. γ as a function of temperature.

The equation listed in Figure 12 is a 4th order polynomial fit to the plotted gamma term and was used in the ANSYS simulation to calculate γ for the effective char thermal conductivity at each timestep. The value of γ and the resulting effective char thermal conductivity (Eq. 3) are both dependent on the temperature, which was calculated as the average temperature of the char elements. To avoid smearing an average effective thermal conductivity across all char elements, the char was split into 10 different layers within the ANSYS model, with a 50 °C temperature limit between layers starting with a temperature limit of 315 °C. Ideally the effective thermal conductivity of the char would be calculated for each element based on the element temperature, but this would not be practical to implement because a unique material number would have to be created for each char element. A foam element was flagged as a char layer if the element temperature reached of 315 °C or higher. The effective thermal conductivity for each char layer is calculated based on the average temperature for that layer.

Table 4 gives a char density of 17.4 kg/m^3. A low-density value for char is conservative during the fire but is non-conservative during the cooldown. Assuming the char density drops to 17.4 kg/m^3 regardless of the initial foam value seems non-conservative during the cooldown when the peak component temperatures typically occur. Assuming the char density equals the foam density is not realistic and would be non-conservative during the fire and overly conservative during the cooldown. A more realistic approach would be to compute the density of the char from the weight percent shown in the TGA curve (Figure 11). The TGA curve plots the weight percent versus temperature but the density cannot be implemented to be dependent on temperature since the density change is permanent and would not revert when the temperature drops. The TGA plots do show that the minimum weight is around 32 percent. The char model

with variable gamma assumes that the effective char density is equal to 32 percent of the initial foam density. Results for the modified ANSYS “char with variable γ” model is shown in Figure 13.

The temperature results in Figure 13 compare reasonably well with the experiment results shown in Figure 2. Probes further away from the heat source (TC8-TC11) under-predicted the temperature compared to the measured results. However, it was noted that during the experiment the foam had moved downward during the test and was restrained by the thermocouple bundles. This downward movement would result in the thermocouples being closer to the heat source than in the model.

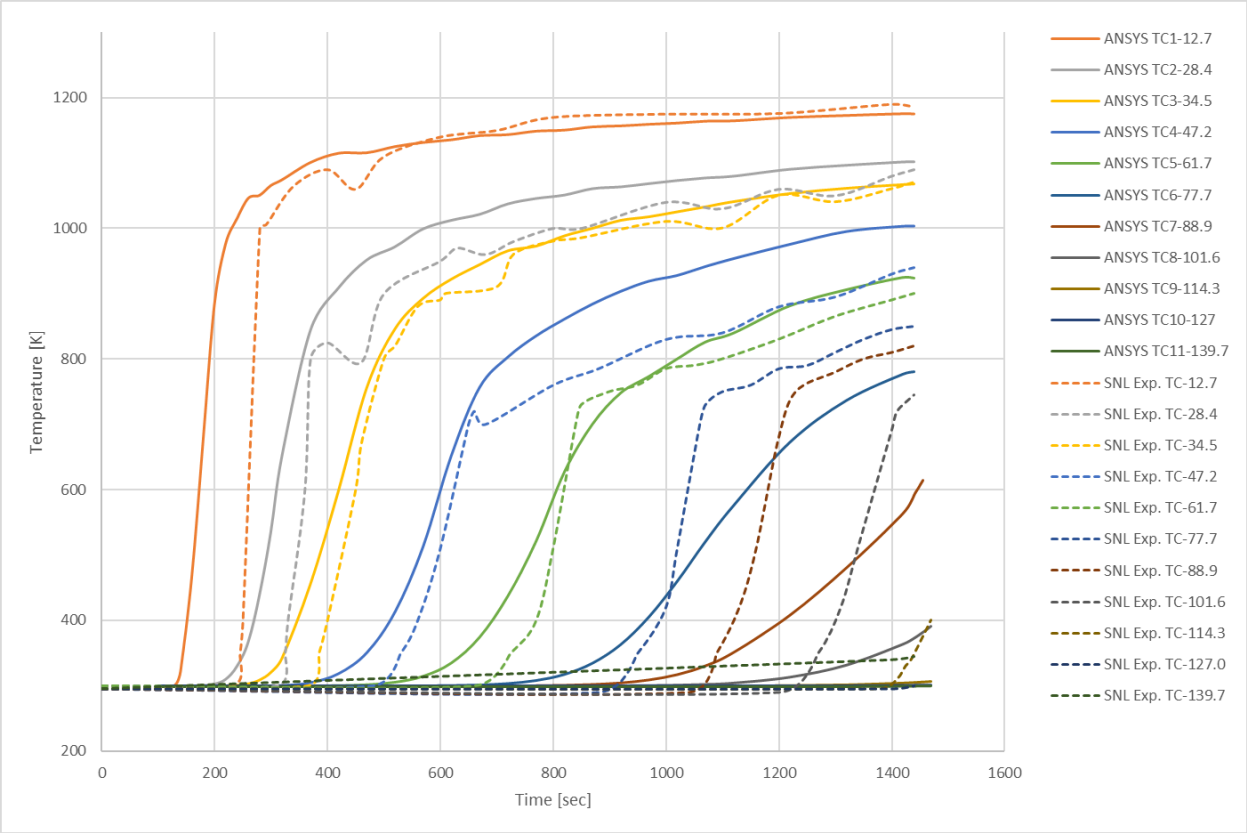

Figure 13. Thermocouple response – “char with variable γ” ANSYS model.

2.6 Char Model with Variable Gamma and Latent Heat

The final case included the latent heat addition associated with the conversion of the condensed phase, virgin foam, to volatiles and solid char. A 577 kJ/kg value cited for transition from a virgin intumescent coating to char by Lautenberger and Fernandez-Pello (2009) was used for the models presented in this paper. To include this latent heat in the ANSYS model, the specific heat of the foam/char layer was increased over the range of expected transition (Eq. 4).

Latent Heat of Volatiles $$\Delta H_{vol} = \int_{T_1}^{T_2} C_{vol} dT$$ Eq. 4

For this case the specific heat was increased from a value of 1640 J/kg-K to 7410 J/kg-K while the layer temperature is between 277ºC and 377ºC.

The addition of the latent heat did not make a significant difference on the resulting temperatures. The resulting thermocouple plot is shown in Figure 14. Thermocouple #1 had the most visible difference, and Figure 15 compares that thermocouple response with and without latent heat. Although the impact of latent heat is small, it is recommended that this feature be included in the completed model and that model sensitivity be tested using latent heat values for GP FR-3700 foams when they are available.

Future models will use the latent heat (heat of reaction) from Pau, et al (2014) that provides a range of values for polyurethane foams. The authors cite a range of values for two pyrolysis reactions, both of which are endothermic. The sum of the two values at the low end of the range, 774 kJ/kg, will be used in future cases (resulting in a specific heat increase from 1640 J/kg-K to 9380 J/kg-K while the layer temperature is between 277ºC and 377ºC). Since the addition of latent heat to the model did not make a significant impact of the resulting temperatures, the cases presented in this paper were not re-run with the higher latent heat value.

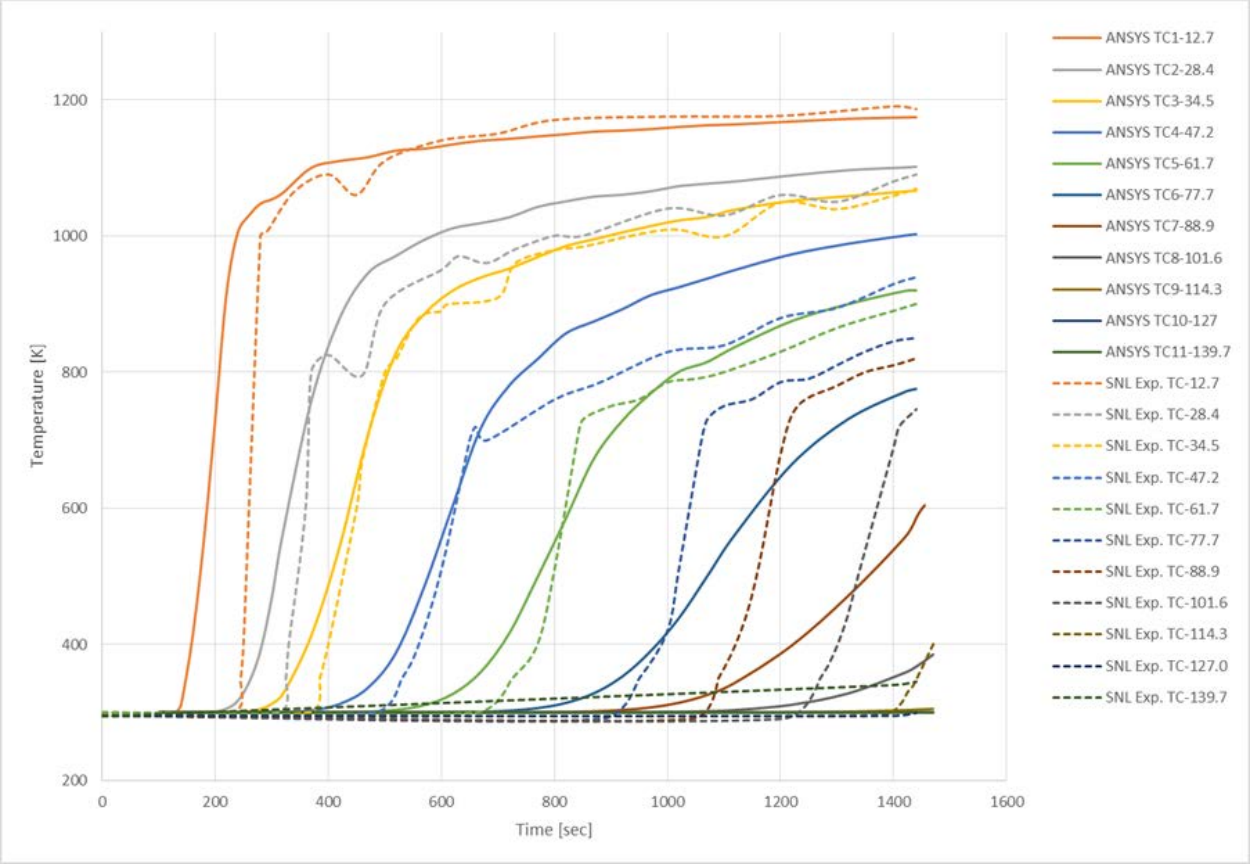

Figure 14. Thermocouple response – “char with variable γ” ANSYS model with latent heat in char layers.

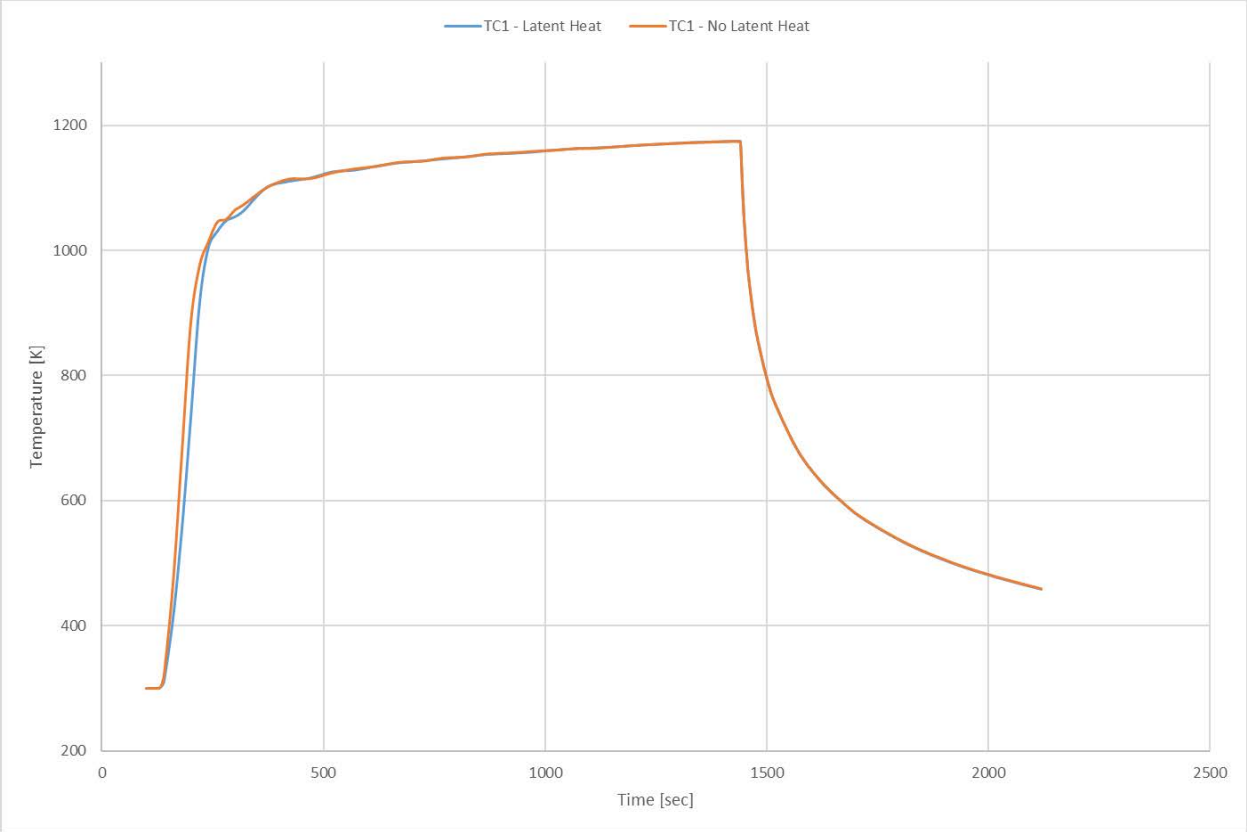

Figure 15. Thermocouple #1 response – "char with variable γ" ANSYS model with and without latent heat in char layers.

In summary, the addition of a layered char model with thermal radiation as a function of foam weight percent is recommended as a path forward for more accurately modeling the thermal response of rigid polyurethane foam exposed to a fire. In the balance of this paper, ANSYS APDL models using the layered char model with variable gamma and latent heat are applied to simulate additional foam degradation experiments and the burn test of an actual package.

2.7 STAR-CCM+ Model with Variable Gamma and Latent Heat

The char model with variable gamma and latent heat was integrated into the STAR-CCM+ model for the SNL Experiment 1. The ANSYS model calculated the effective thermal conductivity of the char layers based on the average temperature of the layer. Ideally the effective thermal conductivity of the char would be calculated for each element based on the element temperature, but this would not be practical to implement in ANSYS because a unique material number would have to be created for each char element. In STAR-CCM+ the effective thermal conductivity of the char layer can be calculated based on the element temperature. The effective char thermal conductivity equation was implemented into STAR-CCM+ through a user defined field function and was calculated for each element (no separate char layers).

Modifying the density and specific heat for the char elements was much more difficult to implement into STAR-CCM+ than ANSYS. The specific heat for the entire Last-A-Foam region (foam and char elements) was continuously calculated based on a volume averaging scheme for the foam and char. Any drastic changes to the density resulted in instability issues when

running the solution. STAR-CCM+ solved physics-based problems using the finite volume method (FVM) versus ANSYS APDL that uses the finite element method (FEM). To account for the density change of the char it was accounted for in the effective thermal conductivity calculation. This was done by adding a multiplier (xF) to the left side term in the effective thermal conductivity equation. The left side term accounts for the conduction heat transfer through the char.

Char Effective Thermal Conductivity $k_{eff} = 0.041(xF)\left(\frac{T}{300}\right)^{0.441} + \gamma(5.670x10^{-8})T^3$ W/m-K

The density effects the heat capacity of the material. In heat transfer analysis the ratio of the thermal conductivity to the heat capacity is termed the thermal diffusivity (α):

$$\propto = \frac{k}{\rho c_p}$$

Where:

- k = thermal conductivity
- c_p = specific heat
- ρ = density

If the char density drops by 32 percent, then the thermal diffusivity increases by a factor of 3.125 (1/0.32):

$$\propto = \frac{k}{0.32\rho c_p} \quad => \quad \propto = \frac{3.125k}{\rho c_p}$$

The rearranged thermal diffusivity equation shows the thermal conductivity (k) multiplied by 3.125 for the lighter char density. From this the xF multiplier is set to 3.125 for all char elements.

The latent heat can also be accounted for in the effective char thermal conductivity equation using an additional multiplier (xCp) over the range from 277 C to 377 C, which is the temperature range over which the specific heat is increased from 1640 J/kg-K to 7410 J/kg-K to account for the transition from foam to char:

$$\propto = \frac{k}{\rho 4.5 c_p} => \propto = \frac{k/_{4.5}}{\rho c_p}$$

The effective thermal conductivity equation for char is updated to incorporate the xCp multiplier:

$$k_{eff} = 0.041(xCp)(xF)\left(\frac{T}{300}\right)^{0.441} + \gamma(5.670x10^{-8})T^3 \quad \text{W/m-K}$$

The xCp multiplier is set to 1/4.5 for char elements initially reaching a temperature of 277 C to 377 C. For temperatures outside of this range, the xCp multiplier is set to 1/1.1 for a char element. This value comes from the specific heat change from 1478 J/kg-K (foam) to 1640 J/kg-K (char). It should be noted that the both the ANSYS and STAR-CCM+ models did not show the latent heat to have a significant impact.

The char model with variable gamma and latent heat was implemented into STAR-CCM+ models for the SNL Experiment 1. Results are presented below in Figure 16 and Figure 17.

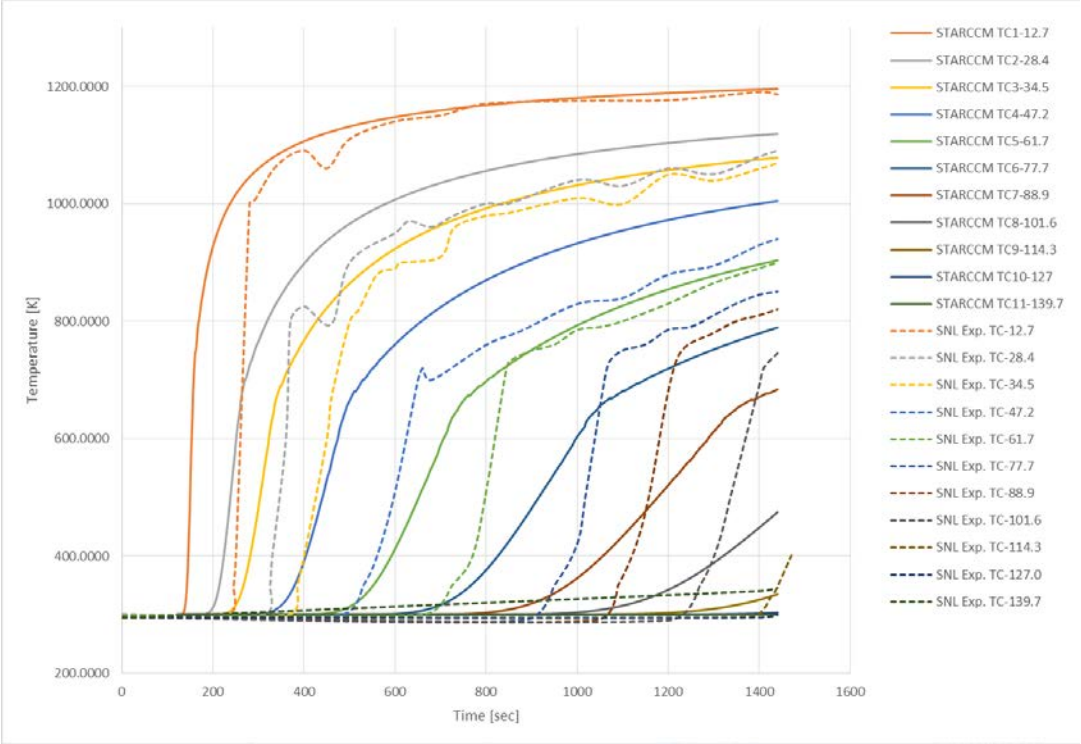

Figure 16. SNL Experiment 1 STAR-CCM+ models.

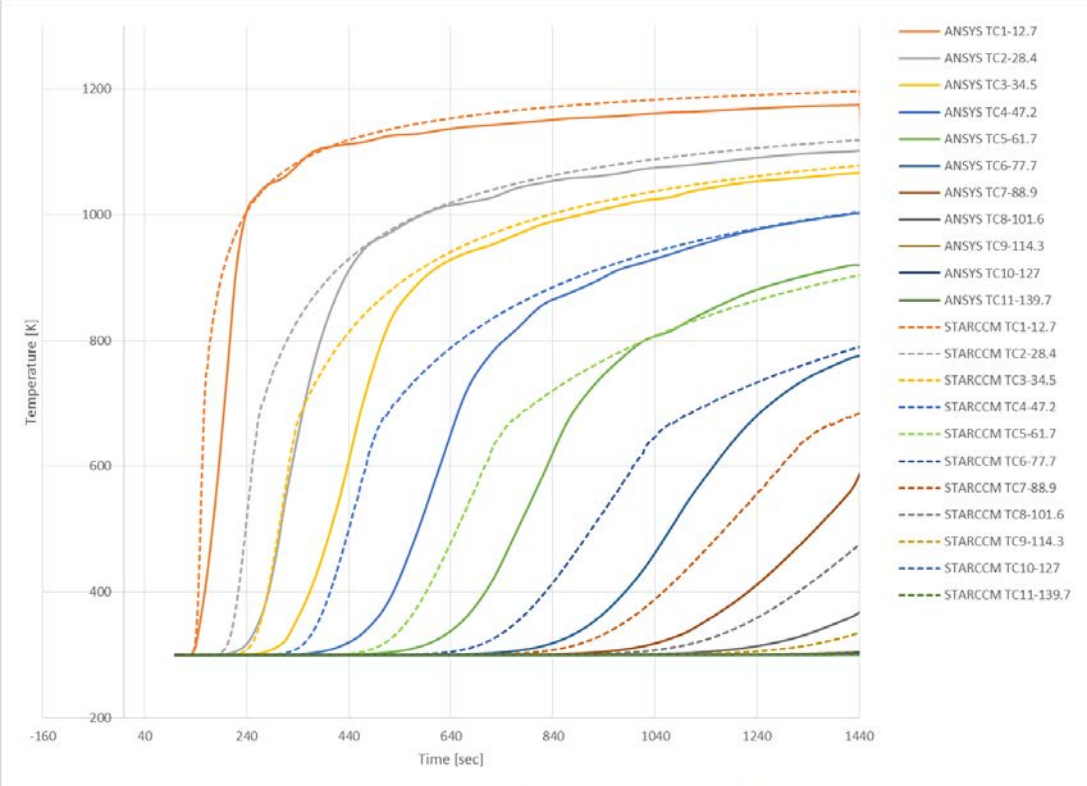

Figure 17. SNL Experiment 1 – comparison of STAR-CCM+ and ANSYS models.

The result plots show the ANSYS and STAR-CCM+ model temperature results are very comparable. Similar to the ANSYS model, the STAR-CCM+ results compare well with the measured thermocouple data for the thermocouples closest to the heated bottom surface but under-predict for those further away from the heated surface.

3.0 SNL Experiment #2

SNL conducted additional fire-induced foam response experiments. These experiments used a higher density foam (22 lb/ft^3, 353 kg/m^3) and considered multiple orientations of the heated surface relative to the foam. Only data for the configuration with the heated surface below the foam sample was included in the reference. The experimental setup and corresponding thermocouple response is shown in Figure 16 (Chu, et al., 1999). This experiment was controlled with a constant heat flux applied to the heated surface of the canister.

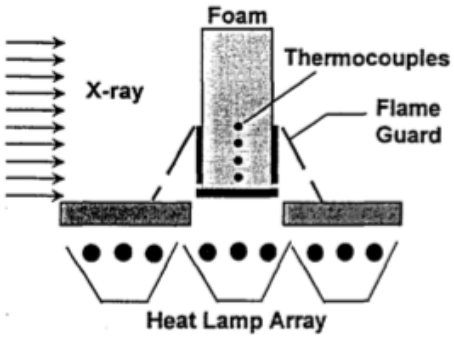

Figure 1 Schematic of ambient pressure vented experiments.

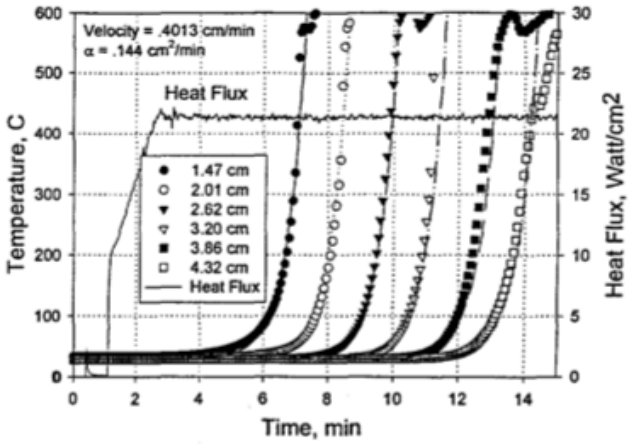

Figure 4 Comparison of experimental results with Landau ablation model for test 5.

Figure 18. Experimental setup and thermocouple response for SNL Experiment #2.

An ANSYS APDL model was constructed to simulate the experimental setup shown in Figure 16. The geometry of the model includes a foam sample (8.76 cm diameter, 14.61 cm long) that sits on top of a 6 mm thick stainless-steel plate, as shown in Figure 17. Both the foam sample and stainless-steel plate are contained within a 7.3 cm long, thin wall (0.5 mm) stainless steel tube (Chu, et al., 1999). Figure 18 shows the meshed geometry for the model. The hybrid hexahedral and wedge element mesh has 639,237 nodes and 618,458 elements.

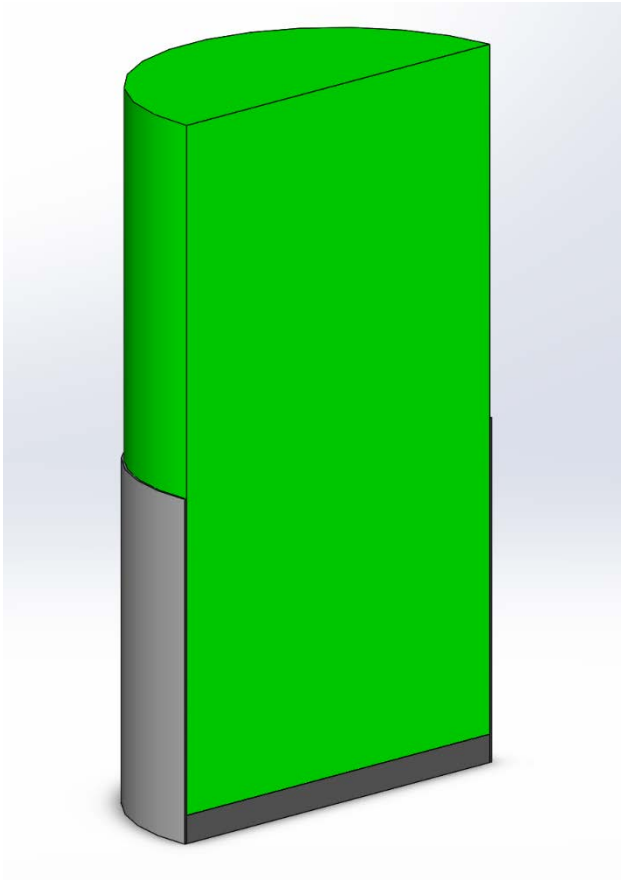

Figure 19. Model geometry for SNL Experiment #2.

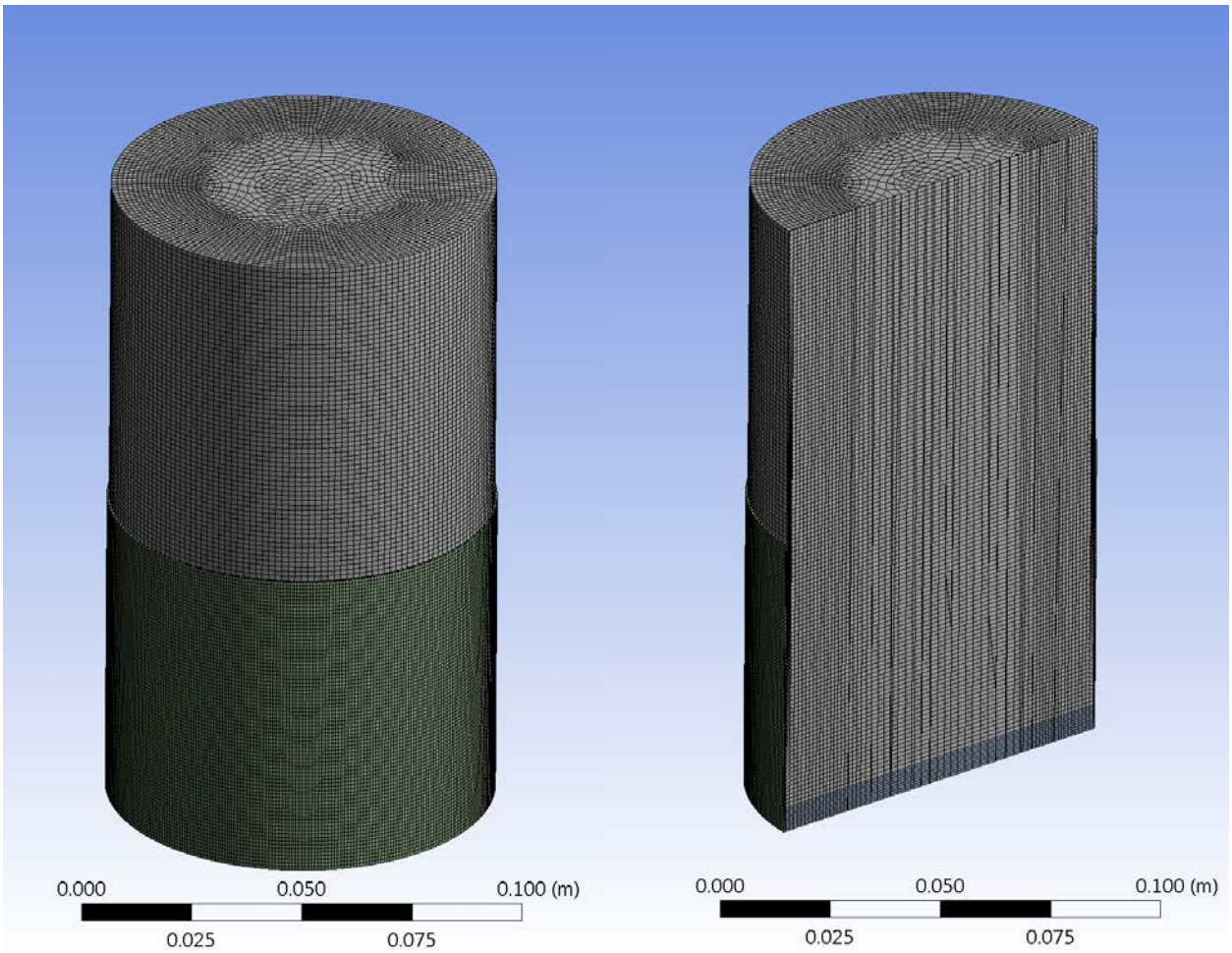

Figure 20. ANSYS APDL mesh of SNL Experiment #2.

The material properties in Table 1 were applied to the stainless-steel plate and tube wall. The emissivities listed in Table 3 were also applied to the SNL Experiment #2 ANSYS model. Material properties used for the higher density polyurethane foam are listed in Table 5.

Table 5. Foam material properties (General Plastics, 1991).

Thermal Conductivity [W/m-K]	Specific Heat [J/kg-K]	Density [kg/m^3]
0.057041	1478	353

Consistent with the experiment, a 212.5 kW/m^2 heat flux boundary was applied along the bottom side of the stainless-steel plate. Natural convection correlations were applied along the externally exposed surfaces of the foam. The correlations used are described in Section 2.1 (Guyer, 1989). The cylindrical sides of the stainless-steel cup were assumed to be adiabatic during heat up. This assumption is based on the proximity of the stainless-steel cup to the radiant heat sources and the flame guard that covers the cup, blocking it from the larger, cooler ambient environment.

Results for the ANSYS APDL model are shown in Figure 19. The predicted timing and rate of temperature increase for the six thermocouple locations compare quite well with the measured data plotted in Figure 21.

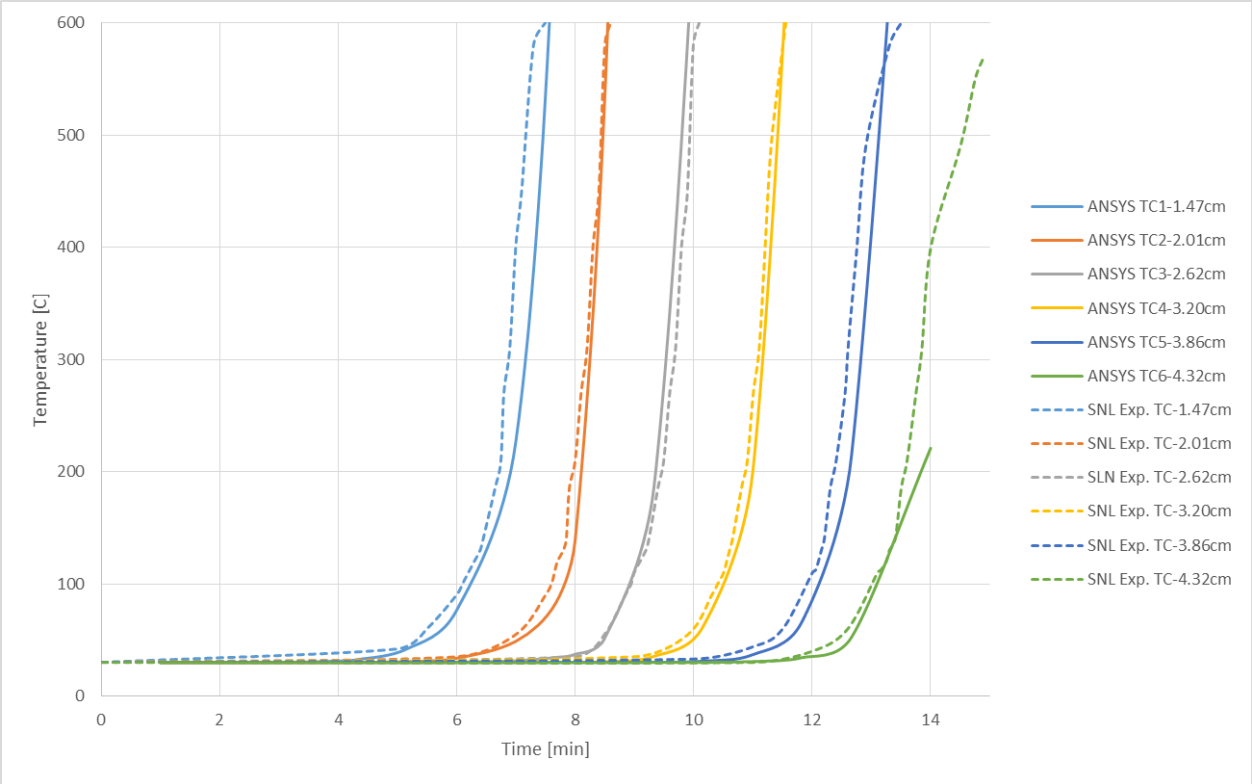

Figure 21. Thermal results for the ANSYS APDL model of SNL Experiment #2.

4.0 SNL Experiment #3

Sandia National Laboratory (SNL) ran an additional experiment similar to experiment # 2 described in Section 3, but in this experiment also included a cylindrical stainless steel component encapsulated within the foam (Hobbs, Erickson, & Chu, 2000). In this experiment the heated foam surface is facing upward, and the experiment was controlled to a set point temperature using a thermocouple in the heated surface. Figure 22 shows a diagram of the experimental setup.

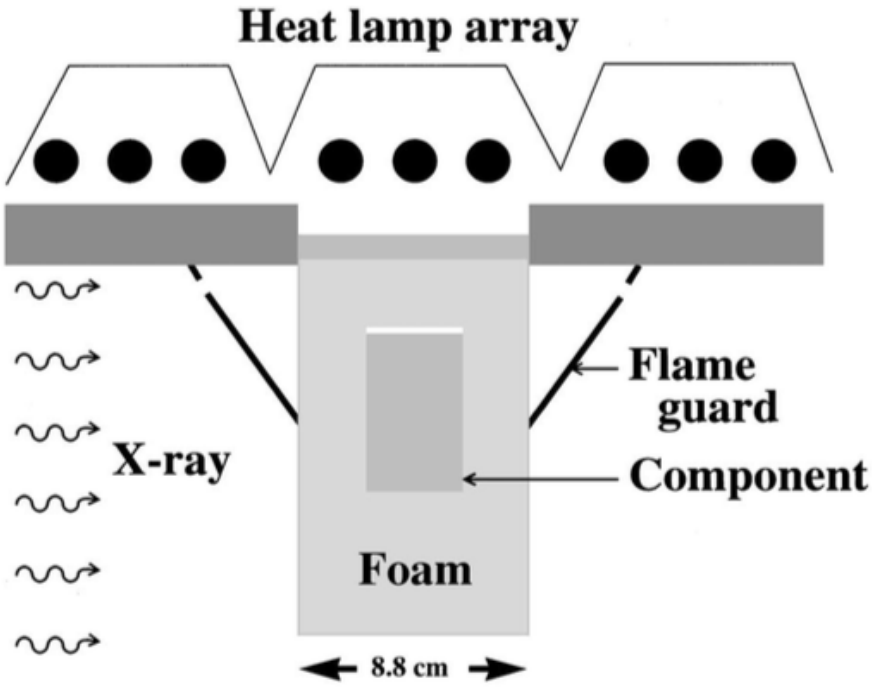

Figure 22. Experimental setup for SNL Experiment #3 (Hobbs, Erickson, and Chu, 2000).

Heat lamps were used to heat a 0.95 cm thick stainless-steel plate up to a temperature of 1000 ºC. Sitting in contact directly below the plate was a 15 cm long foam cylinder with an 8.8 cm diameter. Both the plate and foam were contained within a thin walled (0.5 mm) 7.3 cm long stainless-steel tube (not shown in the diagram in Figure 22, for clarity). Encapsulated within the foam was a 3.8 cm diameter by 6.4 cm long stainless-steel component, as shown in Figure 20. The component was located 3.2 cm from the heated surface. A 3 mm air gap was located directly above the component. Thermocouples were attached to the stainless-steel cup to measure the outer boundary temperatures. These outer wall temperature measurements are shown in Figure 23.

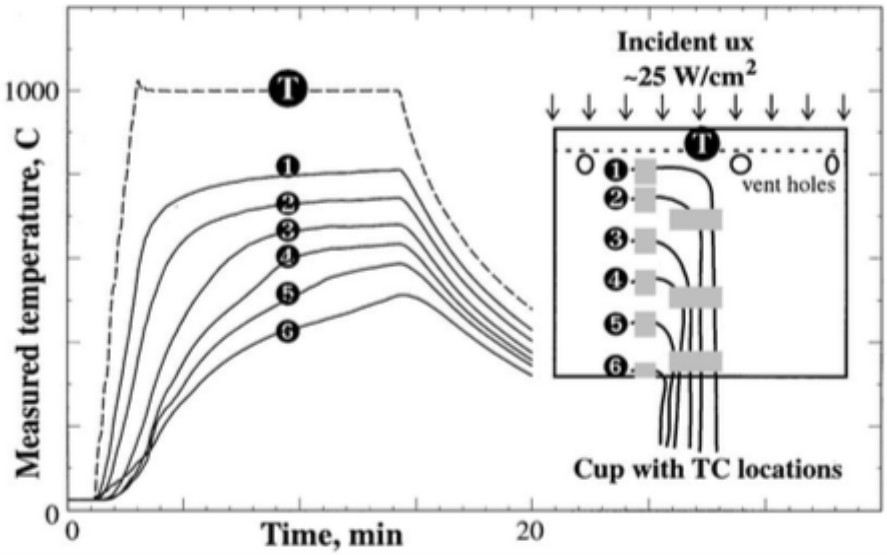

Figure 23. Measured cup wall temperatures and top cup temperature (Hobbs, Erickson, and Chu, 2000).

Thermocouples were also positioned within the foam and at the centerline of the stainless-steel component. The approximate locations of the thermocouples and a comparison of measured temperatures with model predictions from this work are shown in Figure 24.

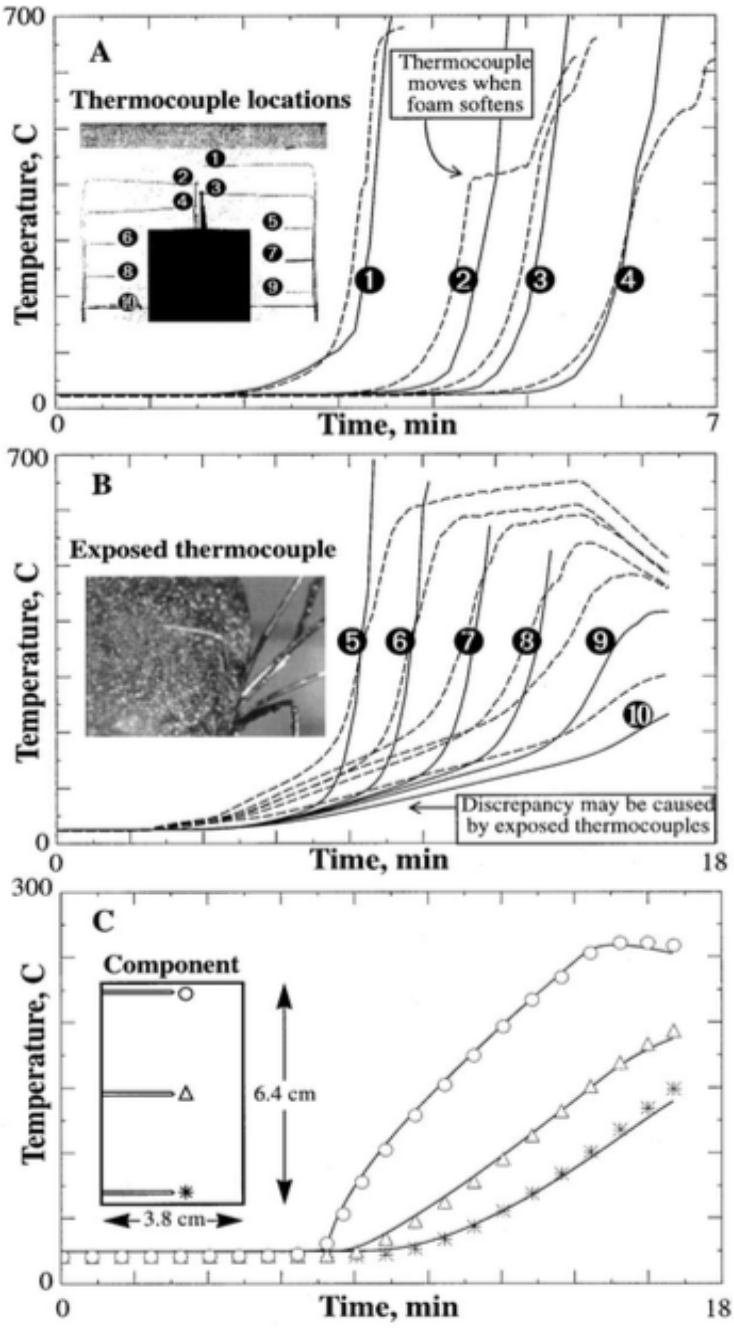

Fig. 15. (A) Calculated (solid lines) and measured (dashed lines) temperatures at various thermocouple locations shown in inset above component, (B) calculated (solid lines) and measured (dashed lines) temperature at various thermocouple locations between 304 SS cylinder and holding cup walls. An exposed thermocouple is shown in the inset which may account for the discrepancy in the measured and calculated temperatures in B. The calculated (lines) and measured (symbols) temperatures of the encapsulated component are shown in C.

Figure 24: Resulting thermocouple temperatures for SNL Experiment #3 (from Fig. 15 of (Hobbs, Erickson, and Chu, 2000)).

An ANSYS APDL model was constructed to simulate the SNL Experiment #3. Figure 23 shows the meshed geometry of the model. The mesh is a hybrid of hexahedral, tetrahedral, and wedge elements. The mesh has a total of 125,595 nodes and 230,843 elements.

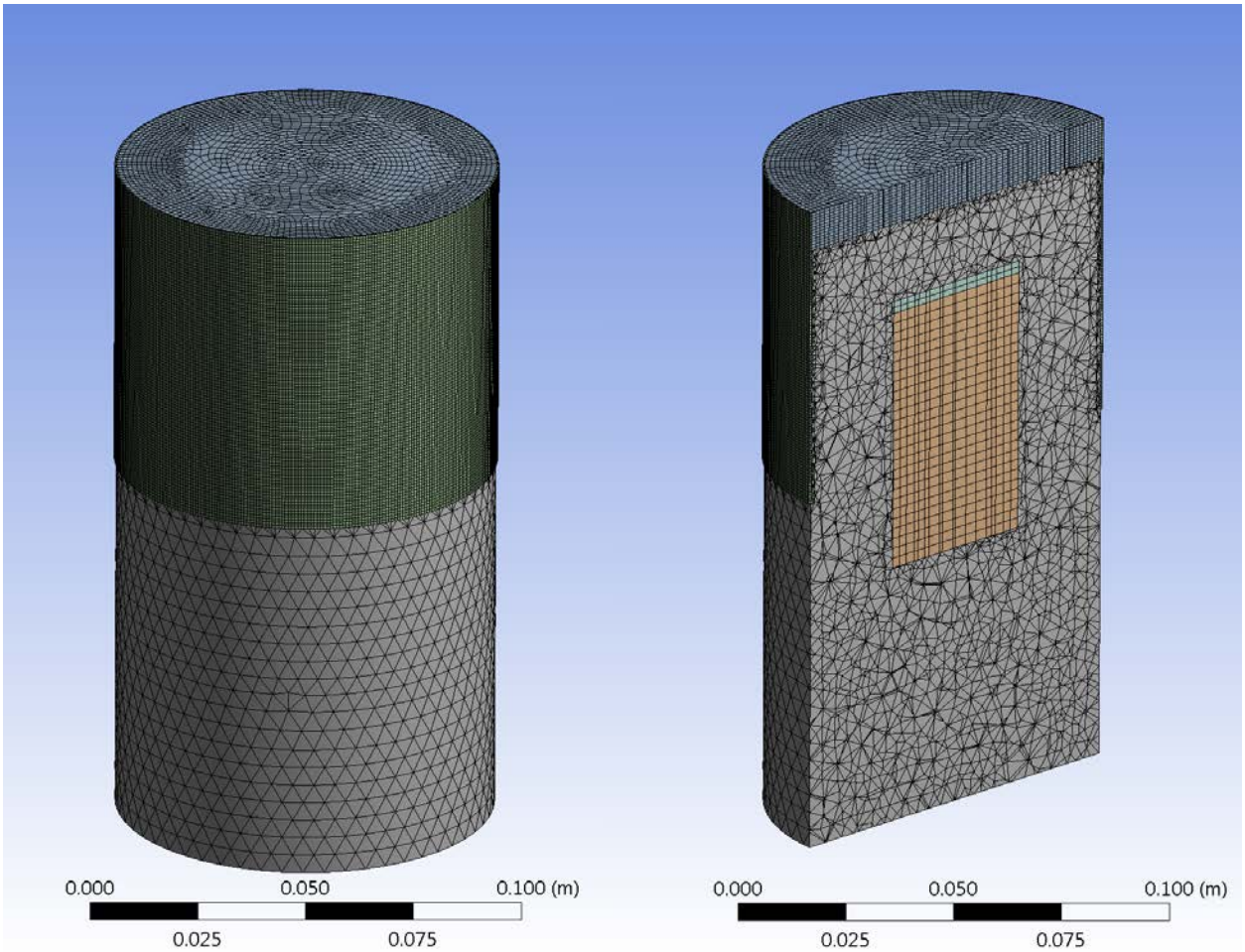

Figure 25. ANSYS APDL mesh of SNL Experiment #3.

Stainless steel material properties listed in Table 1 and the emissivities listed in Table 3 were applied to the SNL Experiment #3 ANSYS model. Temperature-dependent thermal properties for the polyurethane foam used in the experiment were measured with a differential scanning calorimeter and a laser flash technique (Hobbs, Erickson, and Chu, 2000). These properties are listed in Table 6.

Table 6. Foam material properties (Hobbs, Erickson, and Chu, 2000).

Temperature [K]	Thermal Conductivity [W/m-K]	Specific Heat [J/kg-K]	Density [kg/m^3]
296	5.86E-02	1268	353
323	6.28E-02	1356	
373	6.69E-02	1498	
423	7.53E-02	1841	
473	8.37E-02	1987	
523	9.20E-02	2201	

A boundary temperature of 1000 ºC was applied to the top of the stainless-steel plate during the heating portion of the transient analysis (the radiant heaters were turned off around the 14-minute mark). Natural convection correlations were applied along the externally exposed surfaces of the foam. The correlations used are described in Section 2.1 (Guyer, 1989). As in the model of SNL Experiment #2, the cylindrical sides of the stainless-steel cup were assumed to be adiabatic during heat up. This assumption is based on the proximity of the stainless-steel cup to the radiant heat sources and the flame guard that covers the cup blocking it. The adiabatic boundary condition is removed once the radiant heaters are turned off since in the test heat would have been escaping through the thin walled tube. During cooldown a natural convection correlation for a vertical cylinder (Guyer, 1989) is applied to the cylindrical sides of the stainless-steel cup.

Temperature results for the ANSYS model are shown in the three plots that make up Figure 24. Model comparisons with measured temperatures on the foam sample centerline ahead of the stainless-steel component are shown in the first plot (see Figure 24 for thermocouple locations). Comparisons to measurements at thermocouple positions in the foam between the component and cup wall are shown in the second plot. Comparisons with measurements at the centerline of the stainless-steel component are shown in the final plot. While some portion of the differences between model predictions and measured temperatures are due to model shortcomings, differences can also be attributed to measurement uncertainty. One example is positional uncertainty for the thermocouples. This is illustrated in the first plot, where thermocouple #2 was believed to have moved as foam softened (Hobbs, Erickson, and Chu, 2000).

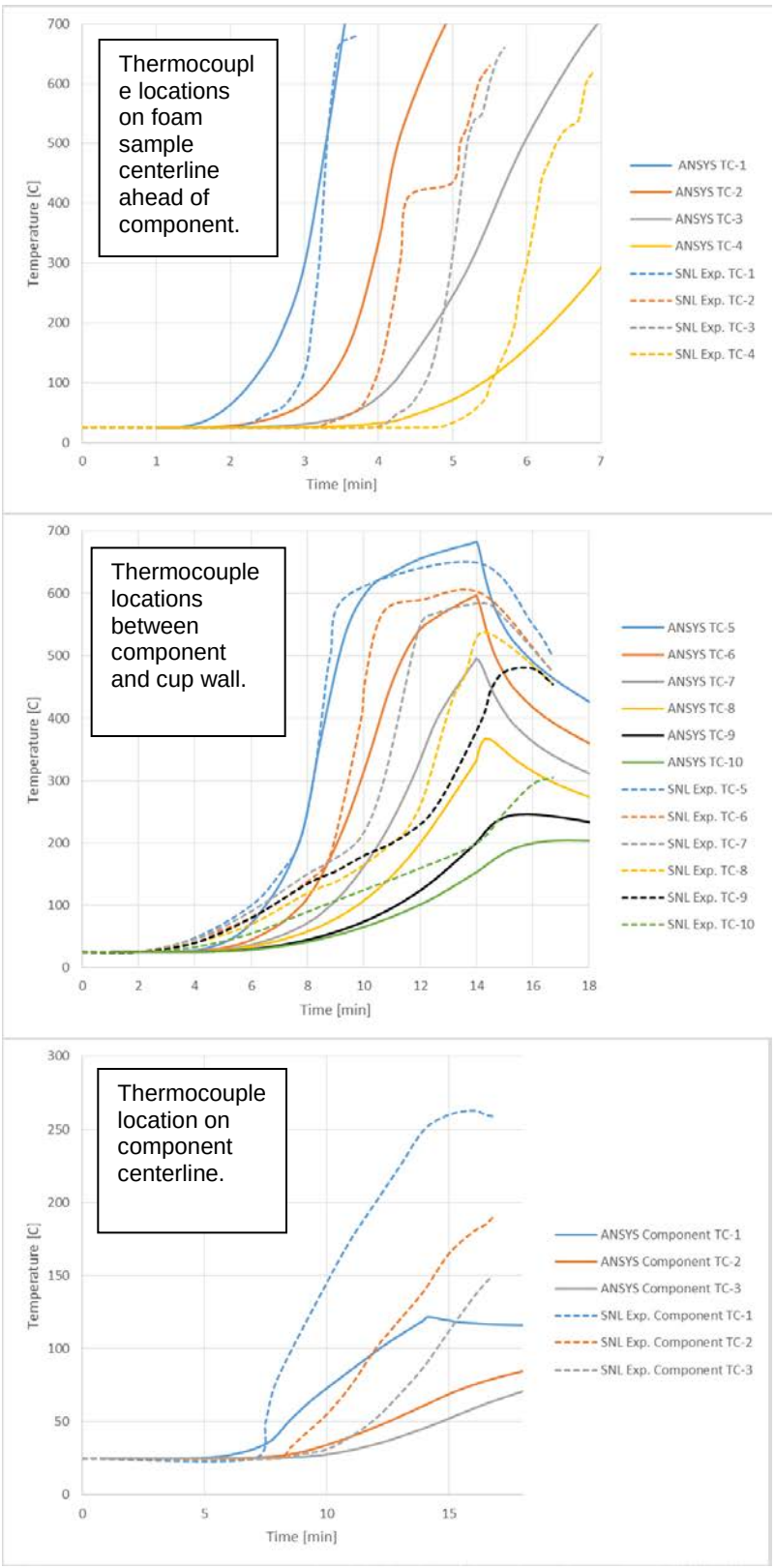

Figure 26. Temperature results for ANSYS APDL model for SNL Experiment #3.

The results in the first two plots of Figure 26 for the thermocouples (TC) located in the foam (TC #1 –TC #10) compare reasonably well with the measured temperatures. In the final plot of Figure 26, the predicted temperatures on the centerline of the stainless-steel component (TC Component #1 – TC Component #3) show the same trend as the measured temperatures shown in Figure 24 but are significantly lower than the measured results. This can be explained by additional physics that are not included in the model. First, the pyrolysis front is complex, including a liquid layer that partially binds the layered char that forms behind (Chu, et al., 1999). Also, in the vertical upward facing geometry of this experiment, the liquid layer reaches the stainless-steel component, enhancing heat transfer, and the char layers collapse and thin out atop the component, exposing it to more direct thermal radiation. These factors all contribute to the difference in model predictions and measured temperature response. This is not expected to be an issue with package models where significant intact foam will surround the contents after an HAC event and where a layer of blanket insulation resides between the foam and drum liner.

5.0 Char Model Applied to 9977 Package

The 9977 package was subjected to a series of burn tests to experimentally examine the thermal response of the package to a HAC fire (SRNL, 2006). The 9977 package is internally filled with a thick layer of Last-A-Foam FR-3716. Four test packages with FR-3716 foam were tested in the SRNL packaging burn test. A practice package with no Last-A-Foam was also burned during the experiment. The 9977 package geometry is shown in Figure 27, with the Last-A-Foam shown in blue.

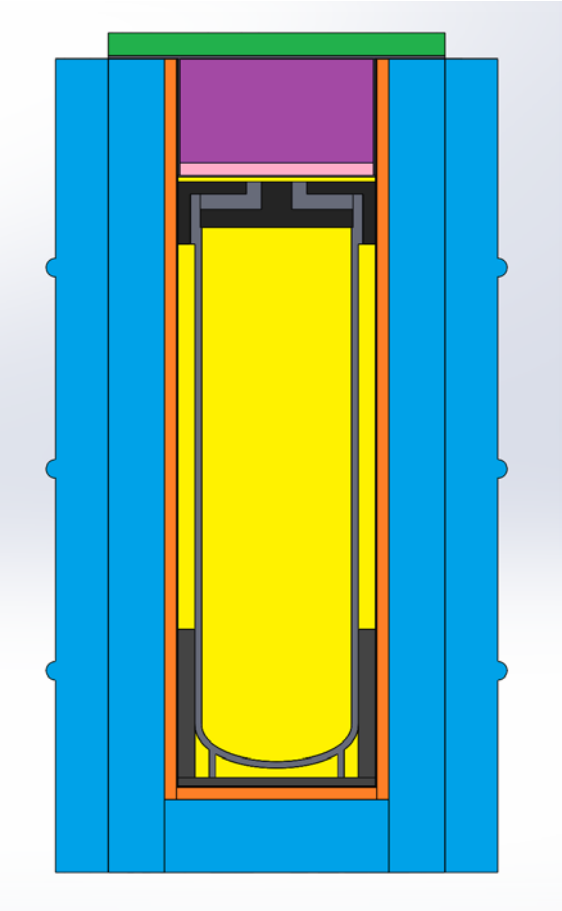

Figure 27. 9977 Package geometry – cross-sectional view through the center of the package.

During the burn tests, the package was equipped with temperature indicators at various locations within the package. Thermocouples were used to capture the flame temperature and the temperature at the outer surface of the package. Table 7 lists the recorded flame and package surface temperatures, and Table 8 lists the measured CV temperatures (SRNL, 2006).

Table 7. SRNL packaging burn test – 30-minute temperature averages (SRNL, 2006).

Test	Package Number	Fire (°C)	Package (°C)
Practice	Practice Package	1014	889
Regulatory Test 1	SN-2	1023	968
Regulatory Test 2	SN-4	848	791
Regulatory Test 3	SN-5	866	995
Regulatory Test 4	SN-3	800	963

Table 8. SRNL packaging burn test – measured CV temperatures.

Table A-1 Indicator Label #	SN-2 Tmax [F]	SN-3 Tmax [F]	SN-4 Tmax [F]	SN-5 Tmax [F]
1	280-290	370-380	420-435	420-435
2	-	290-320	280-290	250-260
3	-	> 500	-	-
4	< 250	260-270	260-270	-
5	-	-	270-280	250-260
6	< 250	260-270	250-260	< 250
7	< 250	260-270	250-260	< 250
8	-	< 250	< 360	< 250
9	< 250	< 250	< 250	< 250
10	-	< 250	<250,<330	< 250
11	< 250	< 250	< 250	< 250
12	< 250	250-260	< 250	< 250
13	250-260	330-340	< 250	< 250
14	< 250	260-270	< 250	< 250
15 - Top	210-220	> 240	> 240	> 240
15 - Middle	210-220	> 240	220-230	220-230
15 - Bottom	-	> 240	210-220	220-230

Both test packages SN-4 and SN-5 were tested in the vertical orientation with the bottom end of the package facing downward. An ANSYS APDL model of the 9977 package was constructed and subjected to a 30 minute fire in the same orientation as the test packages. The SN-4 package burn test experienced fuel feed problems, but this was corrected for the SN-5 package burn test. Therefore, the ANSYS APDL model used the flame and ambient temperature from the SN-5 test to model the package burn experiment. Results from the ANSYS APDL model and comparisons with the measured data from SN-5 package are shown in Table 9. The resulting ANSYS APDL model temperatures compare reasonably well with the measured experiment temperatures. The char model does produce higher peak component temperatures, indicating the model is conservative.

Table 9. ANSYS APDL model temperature results compared with measured data for SN-5.

Temperature Indicator Label #	ANSYS Model Tmax [F]	Measured Data Tmax [F]
1	384.20	420-435
2	264.75	250-260
3	516.48	-
4	264.72	-
5	264.72	250-260
6	264.71	< 250
7	264.76	< 250
8	239.31	< 250
9	239.14	< 250
10	231.99	< 250
11	231.95	< 250
12	231.83	< 250
13	231.77	< 250
14	282.07	< 250
15 - Top	264.72	> 240
15 - Middle	239.14	220-230
15 - Bottom	231.76	220-230

The SRNL experiment also did a post fire examination of two of the packages, SN-2 and SN-3, to determine the amount of foam remaining after the HAC fire. The drum was opened up and all char was removed, leaving only the intact foam. It was determined that approximately 2.3 inches of foam remained around the drum liner and Fiberfrax after the HAC fire (SRNL, 2006). Figure 28 shows the char and remaining foam elements for the ANSYS APDL model after the HAC fire. A ring of foam with a width of ~1.55 inches remains around the vertical sides of the thermal blanket for the model. There is very little foam remaining on the underside of the thermal blanket. This indicates that the model predicted higher temperatures than the experiment and is a conservative representation of the foam degradation. One reason for this discrepancy between the model and experiment could be that in the experiment the package sat on a metal grill plate, which would have provided some shielding from the engulfing fire at the bottom of the package. This grate was not included in the ANSYS APDL model.

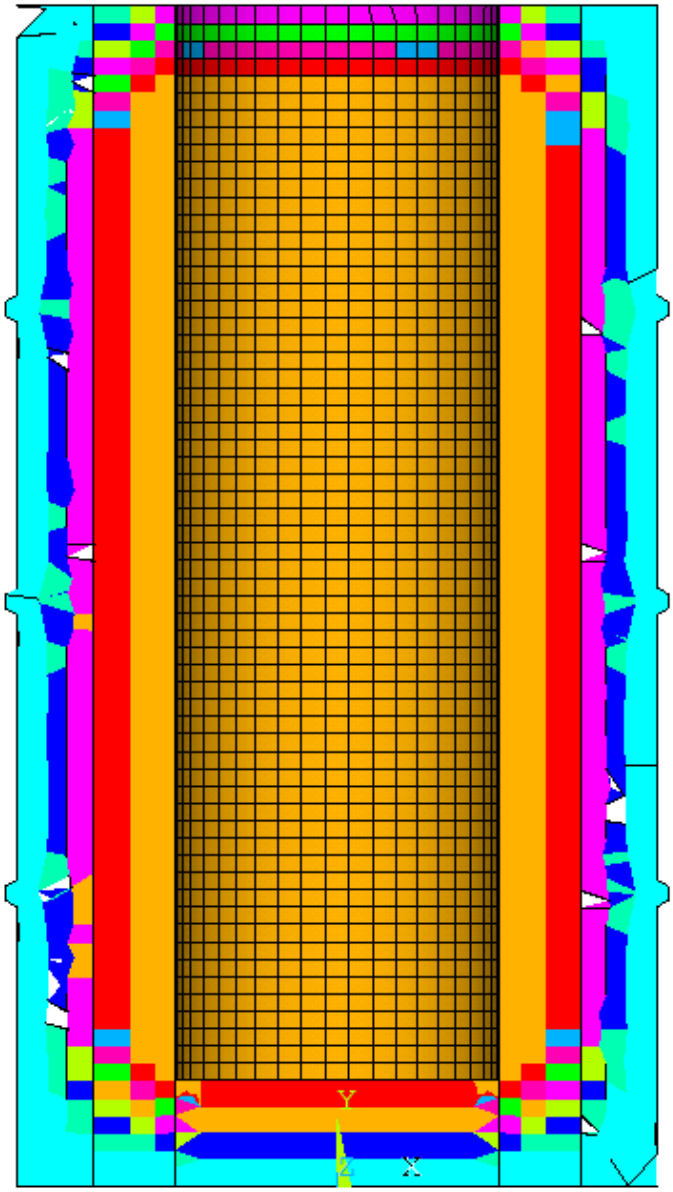

Figure 28. Remaining foam and char elements after the HAC fire and cooldown (remaining foam elements shown in orange).

5.1 STAR-CCM+ Model for 9977

The char model was integrated into a STAR-CCM+ model for the 9977 burn test. Results are presented below in Table 10 and Figure 29.

Table 10. 9977 STAR-CCM+ model.

Thermocouple Label #	STARCCM Model Tmax [F]	Measured Data Tmax [F]
1	328.52	420-435
2	295.54	250-260
3	612.61	-
4	295.39	-
5	295.53	250-260
6	295.41	< 250
7	295.51	< 250
8	268.89	< 250
9	268.87	< 250
10	253.26	< 250
11	253.27	< 250
12	252.59	< 250
13	257.52	< 250
14	330.23	< 250
15 - Top	252.59	> 240
15 - Middle	268.87	220-230
15 - Bottom	295.55	220-230

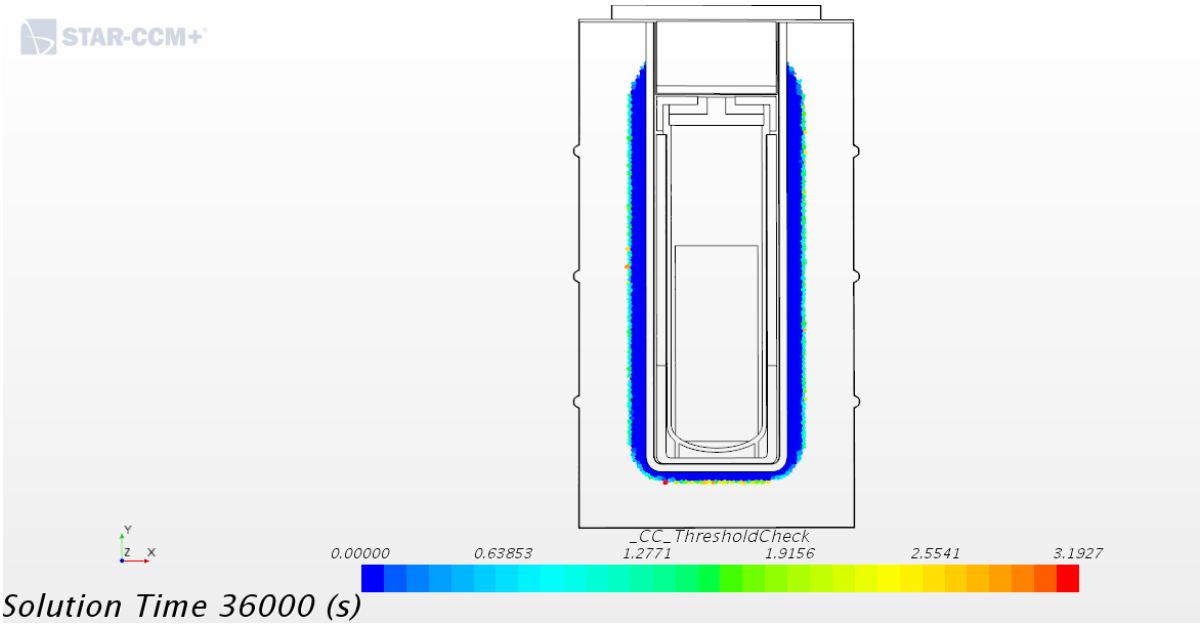

Figure 29. STAR-CCM+ model – remaining foam elements.

The resulting table shows that the STAR-CCM+ model is over predicting at some of the temperature indicator locations. This indicates the STAR-CCM+ model is conservative. The model is predicting a 1.26-inch-thick layer of foam remaining along the sides of the CV and a 0.78-inch-thick layer remaining along the underside of the CV.

6.0 Conclusions and Recommendations

This study set out to find a predictive modeling strategy for rigid polyurethane foam material property changes under HAC thermal conditions, to provide accurate and defensible thermal analysis results. The major results and conclusions of this study are:

- A new model with an effective thermal conductivity based on foam to char density variation was shown successful in representing laboratory-scale foam thermal degradation experiments and full-scale burn tests of a current package.
- This model offers a technically defensible and predictive approach for modeling thermal degradation of rigid polyurethane insulation of Office of Packaging and Transportation (OPT) transport packages.

It is recommended that comparisons with future package HAC thermal tests be conducted as these datasets become available. The DPP-3 is planned for a HAC furnace test in 2020 and this will be a good opportunity to compare model predictions with temperatures and GP foam degradation results.

7.0 References

Chu, T. Y., Gill, W., Moore, J. W., Hobbs, M. L., Gritzo, L. A., & Moya, J. L. (1996). *Experimental Characterization of Fire-Induced Response of Rigid Polyurethan Foam.* Anaheim, CA: 41st International SAMPE Symposium and Exhibition.

Chu, T. Y., Hobbs, M. L., Erickson, K. L., Ulibarri, T. A., Renlund, A. M., Gill, W., Humphries, L. L., Borek, T. T. (1999). *Fire-induced Response in Foam Encapsulants.* Albuquerque, NM: Sandia National Laboratories.

General Plastics. (1991). *General Plastics Last-A-Foam FR-3700 for Crash & Fire Protection of Nuclear Material Shipping Containers.* Tacoma, WA: General Plastics Manufacturing Company.

Guyer, E. (1989). *Handbook of Applied Thermal Design.* New York: McGraw-Hill.

Hobbs, M. L., Erickson, K. L., & Chu, T. Y. (2000). Modeling decomposition of unconfined rigid polyurethan foam. *Polymer Degradation and Stability*, 47-66.

Incropera, F. P., Dewitt, D.P., Bergman, T. L., Lavine, A. S. (2007). *Fundamentals of Heat and Mass Transfer.* New Jersey: John Wiley & Sons, Inc.

Lautenberger, C., & Fernandez-Pello, C. (2009). *Generalized pyrolysis model for combustible solids.* Fire Safety Journal 44.

Litovsky, E., Issoupov, V., Kleiman, J., Latham, R., Kotrba, A., & Olivier, K. (2008). Thermal conductivity of mechanically compressed fiber insulation materials in a wide temperature range: New test method and experimental results. *Proceedings of the 29th International Thermal Conductivity Conference, ITCC29 and the Proceedings of the 17th International Thermal Expansion Symposium, ITES17*, (pp. 283-291).

Pau, D., C. Fleishmann, M. Spearpoint and K. Li. 2014. *Sensitivity of Heat of Reaction for Polyurethane Foams*. In Fire Safety Science, Proceedings of the Eleventh International Association for Fire Safety Science/ DOI: 10:3801/IAFSS.FSS.11-179.

Siemens. (2016). *STAR-CCM+ Users Guide, version 11.06.* Siemens Product Lifecycle Management Software, Inc.

SRNL. (2006). *Safety Analysis Report For Packaging Model 9977.* Aiken, SC: Department of Energy.

Pacific Northwest National Laboratory

902 Battelle Boulevard
P.O. Box 999
Richland, WA 99354
1-888-375-PNNL (7665)

www.pnnl.gov